Published for SISSA by Springer

Received: *February 23, 2020*
Accepted: *May 12, 2020*
Published: *June 10, 2020*

Measurement of the cross section for electroweak production of a Z boson, a photon and two jets in proton-proton collisions at $\sqrt{s} = 13$ TeV and constraints on anomalous quartic couplings

The CMS collaboration

E-mail: cms-publication-committee-chair@cern.ch

Abstract: A measurement is presented of the cross section for electroweak production of a Z boson and a photon in association with two jets ($Z\gamma jj$) in proton-proton collisions. The Z boson candidates are selected through their decay into a pair of electrons or muons. The process of interest, electroweak $Z\gamma jj$ production, is isolated by selecting events with a large dijet mass and a large pseudorapidity gap between the two jets. The measurement is based on data collected at the CMS experiment at $\sqrt{s} = 13$ TeV, corresponding to an integrated luminosity of 35.9 fb^{-1}. The observed significance of the signal is 3.9 standard deviations, where a significance of 5.2 standard deviations is expected in the standard model. These results are combined with published results by CMS at $\sqrt{s} = 8$ TeV, which leads to observed and expected respective significances of 4.7 and 5.5 standard deviations. From the 13 TeV data, a value is obtained for the signal strength of electroweak $Z\gamma jj$ production and bounds are given on quartic vector boson interactions in the framework of dimension-eight effective field theory operators.

Keywords: Electroweak interaction, Hadron-Hadron scattering (experiments)

ArXiv ePrint: 2002.09902

https://doi.org/10.1007/JHEP06(2020)076

JHEP06(2020)076

Contents

1 Introduction **1**

2 The CMS detector **2**

3 Signal and background simulation **2**

4 Object reconstruction and event selection **4**

4.1 Objects reconstruction 4

4.2 Event selection 6

5 Background estimation **8**

6 Systematic uncertainties **8**

7 Results **11**

7.1 Measurement of the signal significance 11

7.2 Fiducial cross section 12

7.3 Limits on anomalous quartic gauge couplings 14

8 Summary **17**

The CMS collaboration **22**

1 Introduction

The standard model (SM) is well tested and continues to be a reliable model of nature, bolstered by the discovery and measurement of the properties of the Higgs boson at the CERN LHC [1–5]. However, a search for incontrovertible evidence of new physics, and a lack of understanding of how all the forces unify motivates further study of the EW sector. For example, novel processes, such as vector boson scattering (VBS), probe unexplored aspects of the nonabelian nature of gauge interactions. The VBS processes are pure electroweak interactions where vector bosons are radiated from the initial state quarks and directly interact via scattering to produce a final state of two scattered vector bosons and two jets from the quarks. Many beyond-the-SM (BSM) models alter the couplings of vector bosons, and such effects can be parametrized through effective field theories [6]. The VBS topology is sensitive to quartic gauge couplings (QGCs) in the SM and to possible anomalous QGCs (aQGCs) [7]. Among all VBS categories, only VBS ZZ and VBS Zγ are sensitive to pure neutral aQGCs. The VBS Zγ has a larger cross section and tight limits are set in this paper.

The EW production of W boson pairs of the same charge was reported by the CMS and ATLAS experiments at $\sqrt{s} = 13\,\text{TeV}$ at respective significances of 5.5 and 6.9 standard deviations [8, 9]. The EW production of WZ bosons was also observed by ATLAS at 13 TeV at a significance of 5.3 standard deviations [10]. Measurements of the EW production cross section of a Z boson and a photon were reported by CMS and ATLAS, based on earlier data collected at 8 TeV, corresponding to respective integrated luminosities of 19.7 and $20.2\,\text{fb}^{-1}$ [11, 12]. The observed significances of these measurements were respectively 3.0

JHEP06(2020)076

and 2.0 standard deviations for CMS and ATLAS, where respective significances of 2.1 and 1.8 standard deviations were expected based on the SM; limits were also reported on the aQGCs. Recently, measurements of the EW production of $Z\gamma$ bosons were updated by ATLAS based on data collected at 13 TeV at a significance of 4.1 standard deviations [13].

We present a study of EW production of $Z\gamma jj$ that includes a measurement of the production cross section and limits on aQGCs at 13 TeV. The data correspond to an integrated luminosity of $35.9 \pm 0.9\,\text{fb}^{-1}$ of proton-proton (pp) collisions collected using the CMS detector in 2016. Candidate events are selected to contain: (i) two identified leptons (electrons or muons) that come from either direct Z boson decay or from indirect Z boson decay through the $Z \to \tau\tau$ chain; (ii) one identified photon; (iii) two jets with a large separation in pseudorapidity (η); and (iv) a large dijet mass. The jet selection reduces the contribution from the non-VBS production of $Z\gamma$, making this signature an ideal topology for VBS studies.

Figure 1 shows representative Feynman diagrams, including (upper left) bremsstrahlung, (upper center) multiperipheral (or nonresonant) production, (upper right) vector boson fusion with trilinear gauge boson couplings (TGCs), (lower left) VBS via a W boson, (lower center) VBS via QGC, and (lower right) quantum chromodynamics (QCD) induced production of $Z\gamma$. The VBS processes are particularly interesting because they involve QGCs (e.g. $WWZ\gamma$). It is not possible, however, to isolate the QGC diagrams from the other contributions that are topologically similar, such as VBS via W boson diagrams. The EW production mechanisms of order α^5 at lowest "tree" level are regarded as signal, and the QCD-induced production mechanisms of order $\alpha^3\alpha_S^2$ at "tree" level are regarded as background, where α and α_S are the respective electromagnetic and strong couplings.

2 The CMS detector

The central feature of the CMS [14] apparatus is a superconducting solenoid of 6 m internal diameter, providing a magnetic field of 3.8 T. A silicon pixel and strip tracker, a lead tungstate crystal electromagnetic calorimeter (ECAL), and a brass and scintillator hadron calorimeter (HCAL), each composed of a barrel and two endcap sections reside within the solenoid volume. Forward calorimeters extend the coverage provided by the barrel and endcap detectors up to pseudorapidities of $|\eta| = 5$. Muons are measured in gas-ionization detectors embedded in the steel flux-return yoke outside the solenoid.

Events of interest are selected using a two-level trigger system [15]. The first level (L1), composed of specialized hardware processors, uses information from the calorimeters and muon detectors to select events of interest with a maximum rate of 100 kHz. A high-level trigger processor farm decreases this rate to 1 kHz before storage. A more detailed description of the CMS detector, together with a definition of the coordinate system and kinematic variables, can be found in ref. [14].

3 Signal and background simulation

The signal and the main background (QCD-induced $Z\gamma jj$) processes are simulated using the respective MadGraph5_aMC@NLO 2.3.3 and 2.6.0 [16] Monte Carlo (MC) generators. The

JHEP06(2020)076

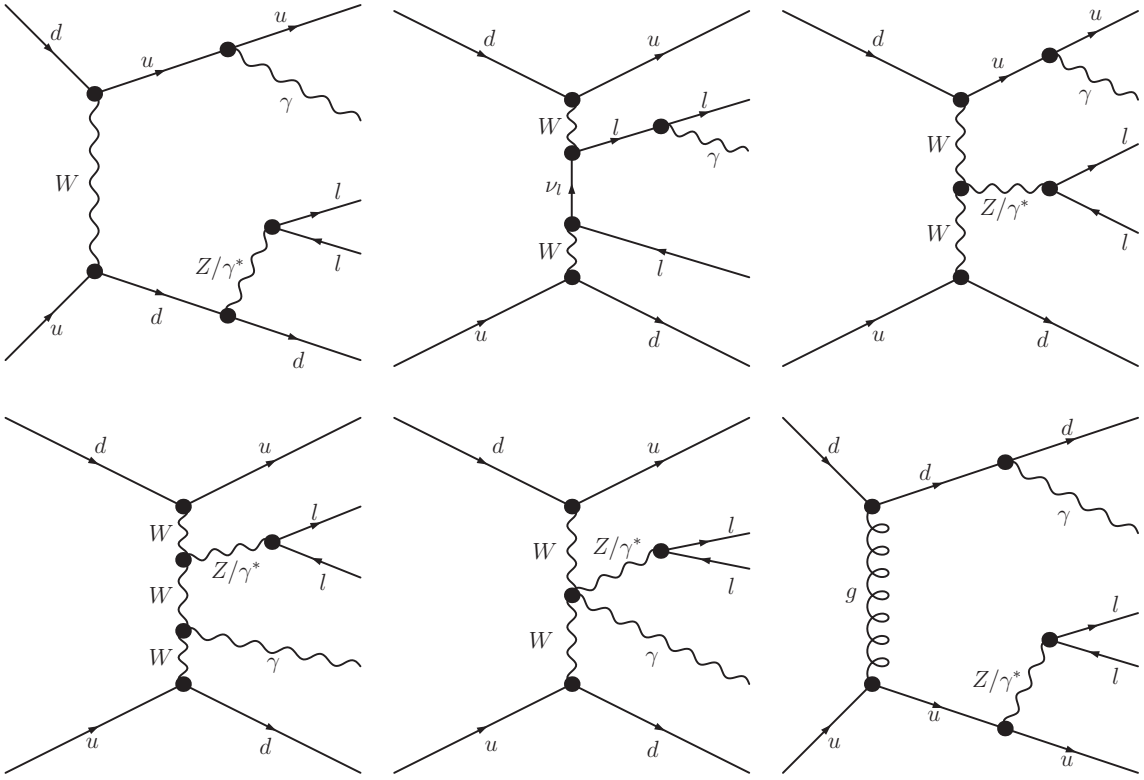

Figure 1. Representative Feynman diagrams for Zγjj production. The diagrams except (lower right) reflect EW origin: (upper left) bremsstrahlung, (upper center) multiperipheral, (upper right) VBF with TGCs, (lower left) VBS via W boson, (lower center) VBS with QGCs, while (lower right) is a QCD-induced diagram.

EW Zγjj signal is simulated at leading order (LO) in QCD, and the QCD-induced Zγjj process simulated at up to one jet in the matrix element calculations at next-to-leading-order (NLO) in QCD, using the FxFx jet merging scheme [17]. The magnitude of the interference is 4–8% depending on m_{jj} and is described in the section on systematic uncertainties. Other background contributions arise from two general classes. The VV backgrounds include QCD-induced Wγjj production simulated at NLO using MadGraph5_aMC@NLO 2.6.0 and diboson processes WW/WZ/ZZ simulated using pythia 8.212 [18]. Top backgrounds include single top quark production simulated at NLO using powheg 2.0 [19–22] and $t\bar{t}\gamma$ production simulated at NLO with MadGraph5_aMC@NLO 2.2.2 using the FxFx jet matching scheme.

The simulation of the inclusion of a aQGC is performed using MadGraph5_aMC@NLO 2.2.2 at LO. The matrix element reweighting feature in MadGraph5_aMC@NLO that provides each event with additional weights corresponding to different theoretical hypotheses, e.g., a different model or a different choice of parameters, is used to extract the size of the coefficients of any anomalous coupling operators probed in the analysis [23].

The pythia 8 generator package using the CUETP8M1 tune is used for parton showering, hadronization, and simulating the underlying event [24, 25]. The NNPDF 3.0 [26] parton distribution functions (PDFs) are used in these studies, and the CMS detector re-

JHEP06(2020)076

sponse in simulated events is modeled using the GEANT4 package [27, 28]. A tag-and-probe procedure [29] is used to measure factors to correct for data-to-simulation differences in trigger, reconstruction, and selection efficiencies. The simulated events include additional pp interactions in the same and neighboring bunch crossings, referred to as pileup (PU). Simulated events are weighted so the PU distribution matches the one from data, with an average PU of ≈23 interactions per bunch crossing.

4 Object reconstruction and event selection

4.1 Objects reconstruction

A particle-flow (PF) algorithm [30] is used to reconstruct particles in the event. It combines all subdetector information to reconstruct individual objects and identify them as charged or neutral hadrons, photons, or leptons (PF candidates).

The reconstructed vertex with largest value in summed object p_{T}^2 defines the primary pp interaction vertex [31] (where p_{T} is the transverse momentum). The objects can also refer to jets clustered using a jet finding algorithm [32, 33] and hadrons assigned to the vertex as inputs. The associated imbalance in transverse momentum in the event ($p_{\mathrm{T}}^{\mathrm{miss}}$) is the magnitude of the vector p_{T} sum of these jets.

Electrons are reconstructed within $|\eta| < 2.5$ for $p_{\mathrm{T}} > 25\,\mathrm{GeV}$. This involves combining the information from clusters of energy deposited in the ECAL and the trajectories fitted in the tracker [34]. The energies of electrons are evaluated from a combination of the electron momentum at the primary interaction vertex determined in the tracker, the energy in the corresponding ECAL cluster, and the energy sum of all bremsstrahlung photons spatially compatible with originating from the electron track. To reduce electron misidentification, electron candidates are required to pass additional identification criteria based on the relative amount of energy deposited in the HCAL, a match of the trajectory in the inner tracker with that in the supercluster [34] of the ECAL, the number of missing hits in the inner tracker, the consistency between the track and the primary vertex, and $\sigma_{\mathrm{i}\eta\mathrm{i}\eta}$, a parameter that quantifies the spread in η of the electromagnetic shower in the ECAL, as discussed in section 5. Electron candidates identified as originating from photon conversions are rejected [34, 35]. Different working points are defined according to their efficiency. The "medium" working point is used to reconstruct electrons in the final state, and a much less restrictive working point, referred to as "veto", is used to reconstruct electrons for vetoing events that contain additional leptons. The medium categories have efficiencies of ≈80% for acceptance of signal and ≈99% for background rejection that change the respective values to 95 and 96% for the veto working point.

Muons are reconstructed from information in the muon system and the inner tracker at $|\eta| < 2.4$ and $p_{\mathrm{T}} > 20\,\mathrm{GeV}$ [36]. The energies of muons are obtained from the curvature of the corresponding tracks. Muon candidates must satisfy identification criteria based on the number of hits in the muon system and the inner tracker, the quality of the combined fit to a track, the number of matched muon-detector planes, and the consistency between the track and the primary vertex. Different working points are defined according to their efficiency. A highly restrictive working point is used to reconstruct muons in the final state,

JHEP06(2020)076

and a far less restrictive working point, referred to as "minimal", is used to reconstruct muons for vetoing events with additional leptons.

Additional cutoffs on relative isolation variables are applied for both electrons and muons. These are defined relative to their p_T values by summing the p_T of the charged hadrons and neutral particles in geometrical cones $\Delta R = \sqrt{(\Delta\eta)^2 + (\Delta\phi)^2} = 0.3$ or 0.4, respectively, about the electrons and muons trajectories:

$$\text{Iso} = \left(\sum p_T^{\text{charged}} + \text{MAX}\left[0, \sum p_T^{\text{neutral}} + \sum p_T^{\gamma} - p_T^{\text{PU}}\right]\right)/p_T,$$

where $\sum p_T^{\text{charged}}$ is the scalar p_T sum of charged hadrons originating from the primary vertex; and $\sum p_T^{\text{neutral}}$ and $\sum p_T^{\gamma}$ are the respective scalar p_T sums of neutral hadrons and photons. The contribution from PU in the isolation cone, i.e., p_T^{PU}, is subtracted using the FastJet technique [33]. For electrons, p_T^{PU} is evaluated using the "jet area" method described in ref. [37]. For muons, p_T^{PU} is assumed to be half of the scalar p_T sum deposited in the isolation cone by charged particles not associated with the primary vertex. The factor of 0.5 corresponds approximately to the ratio of neutral to charged hadrons produced in the hadronization of PU interactions. Electrons are considered isolated when the respective working points for medium and veto are set to Iso < 0.0695 or < 0.175 in the barrel, or Iso < 0.0821 or <0.159 in the endcap detector regions. Muons are considered isolated when Iso < 0.15 or <0.25 for the respective highly restrictive and minimal working points.

Photon reconstruction and selections are similar to those for electrons, and performed in the region of $|\eta| < 2.5$ [38] and $p_T > 20\,\text{GeV}$, excluding the ECAL transition region of $1.444 < |\eta| < 1.566$. The energies of photons are obtained from the ECAL measurements. Photons located in the barrel region, $0 < |\eta| < 1.444$ and the endcap ECAL region, $1.566 < |\eta| < 2.5$, will be referred to as γ_{barrel} and γ_{endcap}, respectively. To minimize photon misidentification, photon candidates are required to pass an electron veto, and satisfy criteria based on the distribution of electromagnetic energy in the ECAL and in the HCAL, and on the isolation variables constructed from the kinematic inputs of the charged and neutral hadrons, and other photon candidates present near the photon of interest. The medium working point is used to reconstruct prompt photons (i.e., not from hadron decays) in the final state, and the minimal working point used to reconstruct nonprompt photons that are mainly products of neutral pion decay [38].

Jets are reconstructed using PF objects and the anti-k_T jet clustering algorithm [32] with a distance parameter of 0.4. The energies of charged hadrons are determined from a combination of their momenta measured in the tracker and the matching of ECAL and HCAL energy deposits, corrected for the response of the calorimeters to hadronic showers. The energy of neutral hadrons is obtained from the corresponding corrected ECAL and HCAL energies. To reduce the contamination from PU, charged PF candidates in the tracker acceptance of $|\eta| < 2.4$ are excluded from jet clustering when they are associated with PU vertices [30]. The contribution from neutral PU particles to the jet energy is corrected based on the projected area of the jet on the front face of the calorimeter. Jets are required to have $p_T > 30\,\text{GeV}$ and $|\eta| < 4.7$. A jet energy correction, similar to the one developed for 8 TeV collisions [39], is obtained from a dedicated set of studies performed

JHEP06(2020)076

on both data and MC events (typically involving dijet, photon+jet, Z+jet and multijet production). Other residual corrections are applied to the data as functions of p_{T} and η to correct for the small differences between data and simulation. Additional quality criteria are applied to jet candidates to remove spurious jet-like features originating from isolated noise patterns in the calorimeters or in the tracker.

4.2 Event selection

Collisions are selected in data using triggers that require the presence of one or two electrons or two muons. The lepton with highest p_{T} is referred to as the leading lepton and denoted $\ell 1$, and the lepton with second-highest p_{T} is referred to as the subleading lepton and denoted $\ell 2$. The p_{T} thresholds for $\ell 1$ and $\ell 2$ in the dilepton triggers are 23 and 12 for electrons, and 17 and 8 GeV for muons. For the single-electron trigger, the p_{T} threshold is 25 GeV. Partial mistiming of signals in the forward region of the ECAL endcap detectors ($2.5 < |\eta| < 3.0$) resulted in L1 triggers being wrongly associated with the previous bunch crossing. Since rules for L1 triggers forbid two consecutive bunch crossings to fire, events with mistimed signals can self veto, which can lead to a significant decrease in L1 trigger efficiency. The loss of efficiency for EW $\mathrm{Z}\gamma\mathrm{jj}$ events associated with the mistiming is $\approx$8% for invariant mass of two jets $m_{\mathrm{jj}} > 500$ GeV, and increases to $\approx$15% for $m_{\mathrm{jj}} > 2$ TeV. This effect is not taken into account in the simulation, and a correction is therefore applied as a function of jet p_{T} and η using an unbiased data sample with correct timing. The correction is implemented through a factor that represents the probability of the event not having mistimed signals.

A selected event is required to have two oppositely charged same-flavor leptons for the reconstruction of a Z boson, i.e., either a pair of electrons or a pair of muons. All leptons used for the Z boson reconstruction must pass the more stringent identification and isolation requirements described in section 4.1. The invariant mass of the dilepton system ($m_{\ell\ell}$) must satisfy $70 < m_{\ell\ell} < 110$ GeV. Events with a third lepton satisfying weaker identification criteria are rejected to reduce background from WZ and ZZ events.

Selected events are also required to contain at least one photon satisfying the identification criteria discussed in section 4.1. The photon with largest p_{T} in the event is used when more than one passes the identification criteria. The ΔR between selected photons and selected leptons is required to be larger than 0.7. The invariant mass of the dilepton-photon system ($m_{\mathrm{Z}\gamma}$) must satisfy $m_{\mathrm{Z}\gamma} > 100$ GeV to reduce the contribution from final-state radiation in Z boson decays. Furthermore, the event must have at least two jets. The jet with largest p_{T} is called the leading jet, referred to as j1, and the jet with second-largest p_{T} is called the subleading jet, referred to as j2. Our selection of jets, leptons, and photons is referred to as the "common" selection.

A low-m_{jj} control region, where the EW signal is negligible compared to QCD-induced $\mathrm{Z}\gamma\mathrm{jj}$ production, is defined by the common selection and the requirement $150 < m_{\mathrm{jj}} < 400$ GeV.

To exploit the unique signature of the VBS process, the leading plus subleading jet system is required to have an invariant mass greater than 500 GeV and an η separation between the jets of $\Delta\eta_{\mathrm{jj}} = |\eta_{\mathrm{j1}} - \eta_{\mathrm{j2}}| > 2.5$. The Zeppenfeld variable [40] $\eta^{*} = |\eta_{\mathrm{Z}\gamma} - (\eta_{\mathrm{j1}} +$

JHEP06(2020)076

Common selection	$p_{\mathrm{T}}^{\ell 1,\ell 2} > 25\,\mathrm{GeV}$, $\lvert\eta^{\ell 1,\ell 2}\rvert < 2.5$ for electron channel
	$p_{\mathrm{T}}^{\ell 1,\ell 2} > 20\,\mathrm{GeV}$, $\lvert\eta^{\ell 1,\ell 2}\rvert < 2.4$ for muon channel
	$p_{\mathrm{T}}^{\gamma} > 20\,\mathrm{GeV}$, $\lvert\eta^{\gamma}\rvert < 1.444$ or $1.566 < \lvert\eta^{\gamma}\rvert < 2.500$
	$p_{\mathrm{T}}^{\mathrm{j1,j2}} > 30\,\mathrm{GeV}$, $\lvert\eta^{\mathrm{j1,j2}}\rvert < 4.7$
	$70 < m_{\ell\ell} < 110\,\mathrm{GeV}$, $m_{\mathrm{Z}\gamma} > 100\,\mathrm{GeV}$
	ΔR_{jj}, $\Delta R_{\mathrm{j}\gamma}$, $\Delta R_{\mathrm{j}\ell} > 0.5$, $\Delta R_{\ell\gamma} > 0.7$
Control region	$150 < m_{\mathrm{jj}} < 400\,\mathrm{GeV}$,
	Common selection
EW signal region	$m_{\mathrm{jj}} > 500\,\mathrm{GeV}$, $\Delta\eta_{\mathrm{jj}} > 2.5$,
	$\eta^{*} < 2.4$, $\Delta\phi_{\mathrm{Z}\gamma,\mathrm{jj}} > 1.9$,
	Common selection
Fiducial region	$m_{\mathrm{jj}} > 500\,\mathrm{GeV}$, $\Delta\eta_{\mathrm{jj}} > 2.5$,
	Common selection, without requirement on $m_{\mathrm{Z}\gamma}$
aQGC search region	$m_{\mathrm{jj}} > 500\,\mathrm{GeV}$, $\Delta\eta_{\mathrm{jj}} > 2.5$,
	$p_{\mathrm{T}}^{\gamma} > 100\,\mathrm{GeV}$,
	Common selection, without requirement on $m_{\mathrm{Z}\gamma}$

Table 1. Summary of the five sets of event-selection criteria used to define events in the common selection, control region selection, EW signal extraction, the fiducial cross section, and the search for an aQGC contribution.

$\eta_{\mathrm{j2}})/2|$, where $\eta_{\mathrm{Z}\gamma}$ is the η of the Zγ system, is required to be < 2.4. The expected recoil between the Zγ and the dijet system, the variable $\Delta\phi_{\mathrm{Z}\gamma,\mathrm{jj}}$, the magnitude of the difference in azimuthal angle between the Zγ and the dijet system, is required to be larger than 1.9. The constraints for η^{*} and $\Delta\phi_{\mathrm{Z}\gamma,\mathrm{jj}}$ are optimized through simulation. This selection defines the EW signal region.

The cross sections for EW Zγjj and EW+QCD Zγjj production are measured in a fiducial region designed to approximate the acceptance of the CMS detector and the signal selection requirements based on the particle-level objects: (i) electrons and muons are required to be prompt, and those from τ lepton decays are excluded; (ii) the momenta of prompt photons with $\Delta R_{\ell\gamma} < 0.1$ are added to the lepton momenta to correct for final-state photon radiation, referred to as "dressing"; (iii) nonprompt photons are excluded; and (iv) VBS-like selections, i.e., $m_{\mathrm{jj}} > 500\,\mathrm{GeV}$ and $\Delta\eta_{\mathrm{jj}} > 2.5$ are required. Additional selections on electrons, muons, photons, and jets are the same as defined in the common selection.

The aQGC search is performed in a region similar to the fiducial region, but with the additional requirement of $p_{\mathrm{T}}^{\gamma} > 100\,\mathrm{GeV}$.

A summary of all the selection criteria for the various regions is shown in table 1.

JHEP06(2020)076

5 Background estimation

The dominant source of background to the EW signal stems from QCD-induced Zγjj production, such as the Feynman diagram in figure 1 (lower right). The estimation of this background comes from simulation, and a simultaneous fit to the control and signal regions is used to constrain the uncertainties affecting its normalization. The uncertainties in the normalization of the QCD-induced Zγjj are significantly smaller after this fit.

A background from events in which the selected photon is not prompt arises mainly from Z+jets production. This background is estimated by applying extrapolation factors to events in a nonprompt photon control sample in data enriched in Z+jets events that corresponds to each region defined in table 1 through just a change in the photon selections. Instead of requiring the photon to pass the identification selection of medium working point, the photon is required to fail that but pass the more relaxed identification selection [12, 41]. The nonprompt extrapolation factors are measured in data in a region similar to our common selection with the jet requirements removed. They are measured as a function of photon p_{T}, photon η, and lepton flavor; the typical variation ranges from 0.1 to 0.5. The numerator in the extrapolation factor is based on a template fit to the distribution in photon $\sigma_{\mathrm{i}\eta\mathrm{i}\eta}$ in data, through which the prompt and nonprompt photon contribution can be easily distinguished from each other. The variable $\sigma_{\mathrm{i}\eta\mathrm{i}\eta}$ quantifies the width of the photon electromagnetic shower in η, which is narrow for prompt and broad for nonprompt photons. The prompt template is obtained from simulated Zγ events and the nonprompt template is obtained from a sideband of charged hadron isolation variable of photon in data. The denominator of the extrapolation factor is simply the number of events in the nonprompt photon control sample, since the contamination of the denominator by prompt photon events is negligible.

Other backgrounds estimated from simulation include single top quark events in the s- and t-channels that are normalized to their respective NLO cross sections; associated single top quark and W boson production normalized to its next-to-next-to-leading order (NNLO) cross section [42]; WW production normalized to its NNLO cross section; WZ, ZZ and QCD-induced Wγjj production normalized to their NLO cross sections; and $\mathrm{t\bar{t}}\gamma$ production normalized to its NLO cross section. All of these processes are also normalized to the integrated luminosity of the data.

After imposing the EW signal region selection, the pre-fit (i.e. before the simultaneous fit) m_{jj} distributions for the dilepton + γ_{barrel} and the dilepton + γ_{endcap} categories described in section 4.2 are shown respectively in figures 2 and 3. The agreement between data and the combined expectation for signal and backgrounds is reasonable.

6 Systematic uncertainties

Systematic uncertainties that affect the measurements arise from experimental issues, such as detector effects and the methods used to compute higher-level quantities, e.g., efficiencies, and variations in theoretical inputs such as the choice of the renormalization and factorization scale and the choice of the PDFs. Each systematic uncertainty is quantified

JHEP06(2020)076

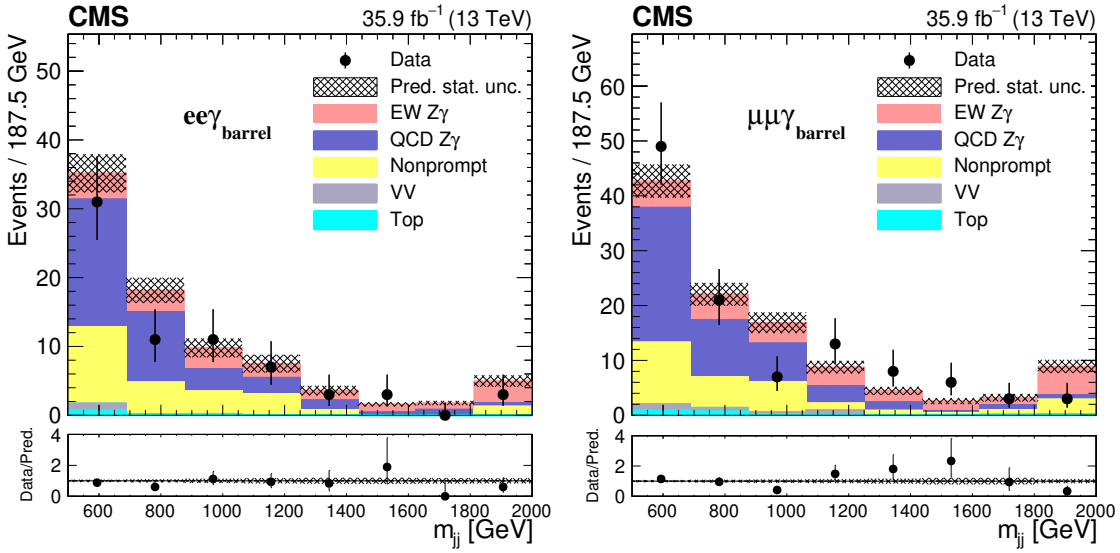

Figure 2. The pre-fit m_{jj} distributions for the dilepton + γ_{barrel} events are shown on the left for the dielectron and on the right for the dimuon categories. The data are compared to the sum of the signal and the background contribution. The black points with error bars represent the data and their uncertainties, while the hatched bands represent the statistical uncertainty on the combined signal and background expectations. The last bin includes overflow events. The bottom plots show the ratio of the data to the expectation.

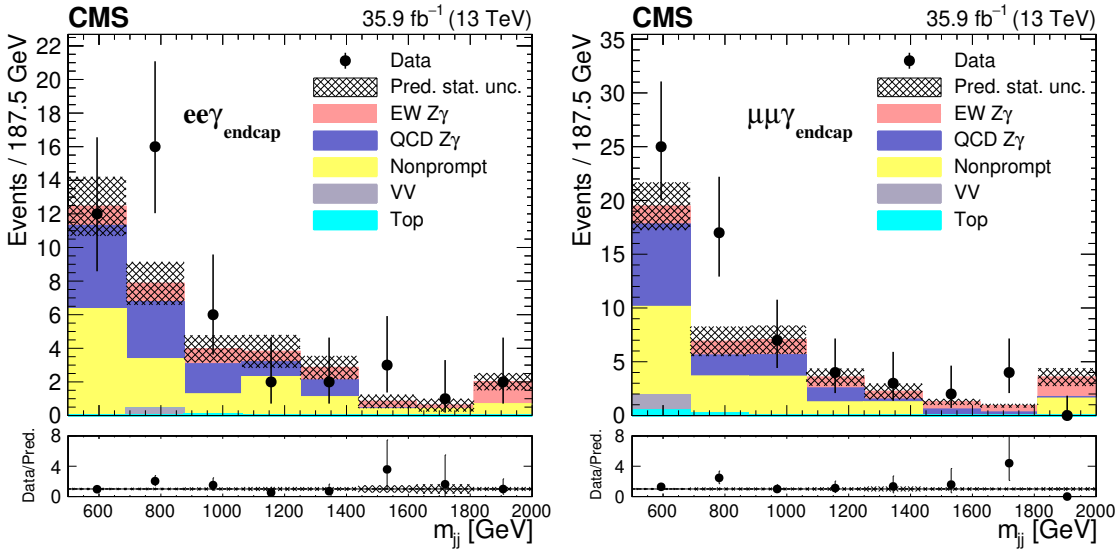

Figure 3. The pre-fit m_{jj} distributions for the dilepton + γ_{endcap} events are shown on the left for the dielectron and on the right for the dimuon categories. The data are compared to the sum of the signal and the background contribution. The black points with error bars represent the data and their uncertainties, while the hatched bands represent the statistical uncertainty on the combined signal and background expectations. The last bin includes overflow events. The bottom plots show the ratio of the data to the expectation.

JHEP06(2020)076

by evaluating its effect on the yield and distribution of relevant kinematic variables in the signal and background categories. The log-normal distribution is used to model the dependence on systematic uncertainties.

The systematic uncertainties in the trigger, lepton reconstruction, and selection efficiencies are measured using the tag-and-probe technique and are 2–3%. The uncertainties in jet energy scale (JES) and jet energy resolution (JER) are calculated from simulated events by rescaling and spreading the jet p_{T}, and propagating the bin-by-bin effects in the variables. The uncertainties from JES and JER vary in the respective ranges of 1–49 and 1–26%. An uncertainty of 2.5% in the integrated luminosity [43] is estimated from simulation. The statistical uncertainties from the size of the number of simulated events as well as the size of data samples used in our background and signal are corrected assuming Poisson distributions, and calculated bin-by-bin. The uncertainties related to the number of simulated events, or to the limited number of events in the data control sample, are respectively 5–46% for the EW Zγjj signal, 10–50% for the QCD-induced Zγjj background, and 20–100% for the nonprompt photon background where the uncertainty value increases with increasing m_{jj} and $\Delta\eta_{\mathrm{jj}}$, and are uncorrelated across different processes and bins of any single distribution. The uncertainties from the correction factors caused by the ECAL mistiming vary by 1–4%, and are applied to all the simulated events and treated as being correlated across different processes and bins.

An overall uncertainty in the nonprompt photon background is estimated through the quadratic sum of systematic uncertainties from several sources. The uncertainty from the choice of isolation variable use in the sideband is estimated through the nonprompt photon fraction for alternative choices of isolation variable sideband [12]. An uncertainty on closure is defined by fits performed to the nonprompt photon fraction in simulated events and comparing the fit results with the known fractions. The closure uncertainty in the region of the endcap detector is larger than in the barrel, and becomes greater with increasing photon p_{T}. This uncertainty provides the dominant part of the systematic component from sources of nonprompt photons. The overall uncertainty in the nonprompt photon background is in the range of 9–37%.

However, theoretical uncertainties have largest impact on the measurement. The scale uncertainty is estimated through simultaneous changes in the μ_{R} and μ_{F} scales up and down by a factor of two relative to their nominal value in each event, under the condition that $1/2 \leq \mu_{\mathrm{R}}/\mu_{\mathrm{F}} \leq 2$. The maximal difference with respect to the nominal value is taken as the measure of uncertainty. The uncertainties in the PDFs are estimated by combining the expectations from all of the contribution in the NNPDF3.0 set of PDFs, according to the procedure described in ref. [44]. For the signal, the scale uncertainty is within the range of 2–14% and the PDF uncertainty within range 3–11% that increases with increasing m_{jj} and $\Delta\eta_{\mathrm{jj}}$. The scale uncertainty in QCD-induced Zγjj events, which has a large impact on the measurement, varies in the range of 5–25%. It is constrained in the simultaneous fit to the signal in the low-m_{jj} control region. The PDF uncertainty in the QCD-induced Zγjj events is in the range of 1–3%.

The interference term between the EW and QCD-induced processes at order $\alpha^4\alpha_{\mathrm{S}}$ at the tree level, is estimated at the particle level using MadGraph5_aMC@NLO. The

JHEP06(2020)076

Source of systematic uncertainty	Relative uncertainty [%]
Scales in QCD-induced Zγjj bkg	5–25
Scales in EW Zγ signal	2–14
Interference	4–8
JES	1–49
JER	1–26
Nonprompt photon bkg	9–37
Integrated luminosity	2.5
L1 mistiming correction	1–4
Photon identification	3
Pileup modeling	1
Trigger and selection efficiency	2–3

Table 2. The pre-fit systematic uncertainties in the measurement of the extracted signal. They are for signal or background (bkg) if the source is specified, or for both if the source is not specified.

interference contribution is defined as the difference between the cross section for inclusive Zγjj production, which contains the interference term, and the sum of the cross sections for pure EW Zγjj and QCD-induced Zγjj. It is positive, and the ratio of the interference to EW Zγjj production that decreases with increasing m_{jj} is in the range of 4–8%, which is consistent with the range obtained from a pure interference term directly generated using MadGraph5_aMC@NLO.

All the above systematic uncertainties are applied to both the measured significance of the signal and to the search for aQGC. They are also propagated to the uncertainty in the measured fiducial cross section, with the exception of the theoretical uncertainties associated with the signal cross section. All systematic uncertainties except those arising from trigger and lepton identification efficiencies are assumed to be correlated between the electron and muon channels. Various sources of systematic uncertainties and their effect on the event yields in the process are summarized in table 2.

7 Results

7.1 Measurement of the signal significance

The post-fit (i.e. after the simultaneous fit) simulated signal and background yields as well as the observed data yields in the EW signal region are listed in table 3.

To quantify the significance of the measured EW Zγ signal, a statistical analysis of the event yields is performed in a two-dimensional (2D) m_{jj} and $\Delta\eta_{\mathrm{jj}}$ grid. There are 4 categories within the signal region that correspond to the choice between barrel and endcap-detector photons and between electron and muon final states. For each bin in m_{jj} and $\Delta\eta_{\mathrm{jj}}$, we construct a Poisson function in the number of observed events. The likelihood is the product of the Poisson distributions for the bin contents and log-normal distributions

JHEP06(2020)076

Processes	eeγ_{barrel}	eeγ_{endcap}	$\mu\mu\gamma_{\text{barrel}}$	$\mu\mu\gamma_{\text{endcap}}$
QCD-induced Zγjj bkg.	39.0 ± 3.0	12.2 ± 1.4	51.1 ± 3.5	14.9 ± 1.5
Nonprompt photon bkg.	23.2 ± 3.0	23.9 ± 3.3	27.1 ± 3.2	28.9 ± 3.8
Other bkgs.	2.2 ± 1.0	0.7 ± 0.5	5.4 ± 1.3	2.5 ± 1.0
Total bkgs.	64.4 ± 4.4	36.8 ± 3.6	83.6 ± 5.0	46.3 ± 4.2
EW Zγjj signal	14.0 ± 1.6	5.0 ± 0.6	20.2 ± 2.3	7.0 ± 0.8
EW signal + total bkgs.	78.4 ± 4.7	41.8 ± 3.7	103.8 ± 5.5	53.3 ± 4.3
Data	69	44	110	62

Table 3. Post-fit signal and background yields and observed event counts in data after the final selection in the search for EW signal. The γ_{barrel} and γ_{endcap} represent photons in the barrel and endcap-detector region, respectively. "Other bkgs." represents the contribution of diboson, top and Wγ process. The uncertainties are the quadratic sum of statistical and systematic uncertainties.

for the uninteresting constraints in "nuisance" parameter. All background contributions are allowed to vary within their associated uncertainties. A p-value that represents the probability to obtain the data given a background-only hypothesis is computed using a profile likelihood-ratio test statistic [45–47]. The p-value is then converted to a significance based on the area in the "tail" of a normal distribution. The post-fit 2D distributions are shown in figures 4 and 5. The binning in m_{jj} and $\Delta\eta_{\text{jj}}$ is optimized for best signal significance. The observed and expected significance for the signal in the data is 3.9 and 5.2 standard deviations with the data set collected in 2016. The main contributions to the significance are from bins with an excess of signal relative to background events, i.e., high m_{jj} bins in each channel. The data in the dimuon + γ_{barrel} and dielectron + γ_{endcap} channels are in good agreement with the expectations in these three bins, while the data are below the expectations in the other two channels. The downward fluctuations of the data in the dimuon + γ_{endcap} and dielectron + γ_{barrel} channels result in the difference between the observed and expected significance. The total uncertainty on the measurement is dominated by the statistical uncertainty in the data. After combining this analysis with the results obtained at 8 TeV [12] using a simultaneous fit, the observed and expected significance becomes, respectively, 4.7 and 5.5 standard deviations. In the combination of the 13 TeV and 8 TeV results, the theoretical uncertainties are treated as correlated because they affect the cross section of the sample and the calculation of the experimental acceptance in the same way, independently of the data-taking period; the experimental uncertainties in the efficiencies of the triggers, object reconstruction and identification are determined independently for each data sample and are uncorrelated.

7.2 Fiducial cross section

A fiducial cross section is extracted using the same m_{jj}–$\Delta\eta_{\text{jj}}$ binnings as used in the calculation of the significance, and through the same simultaneous fit used in the control region. The fiducial region is defined in table 1. We define the cross section as

$$\sigma^{\text{fid}} = \sigma_{\text{g}} \hat{\mu} \text{a}_{\text{gf}},$$

JHEP06(2020)076

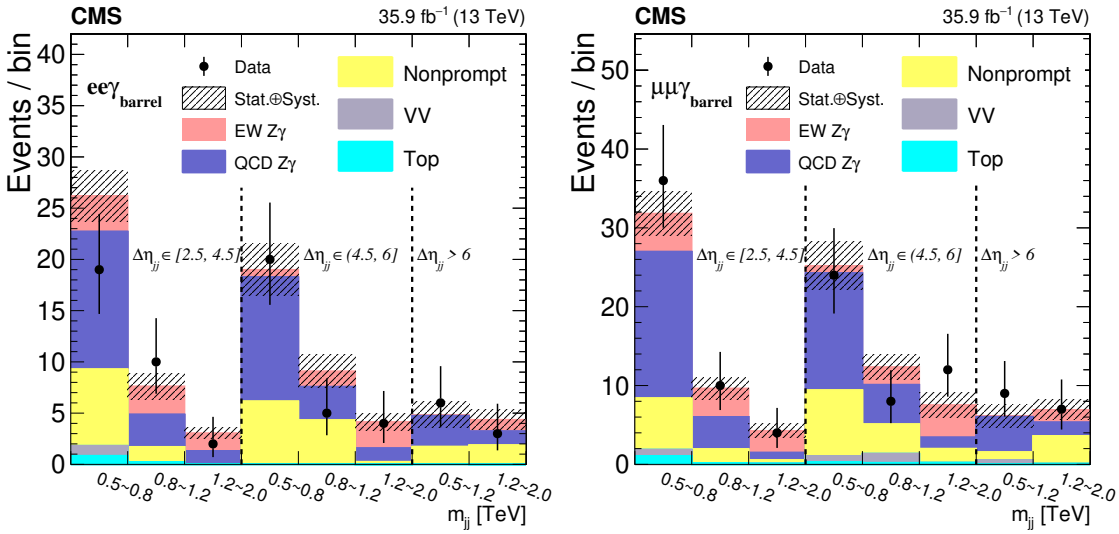

Figure 4. The post-fit 2D distributions of the dielectron (left) and dimuon (right) + γ_{barrel} categories as a function of m_{jj} in bins of $\Delta\eta_{\text{jj}}$. The horizontal axis is split into bins of $\Delta\eta_{\text{jj}}$ of [2.5, 4.5], (4.5, 6.0], and > 6.0. The data are compared to the signal and background predictions in the signal region. The black points with error bars represent the data and statistical uncertainties of data, the hatched bands represent the full uncertainties of the predictions.

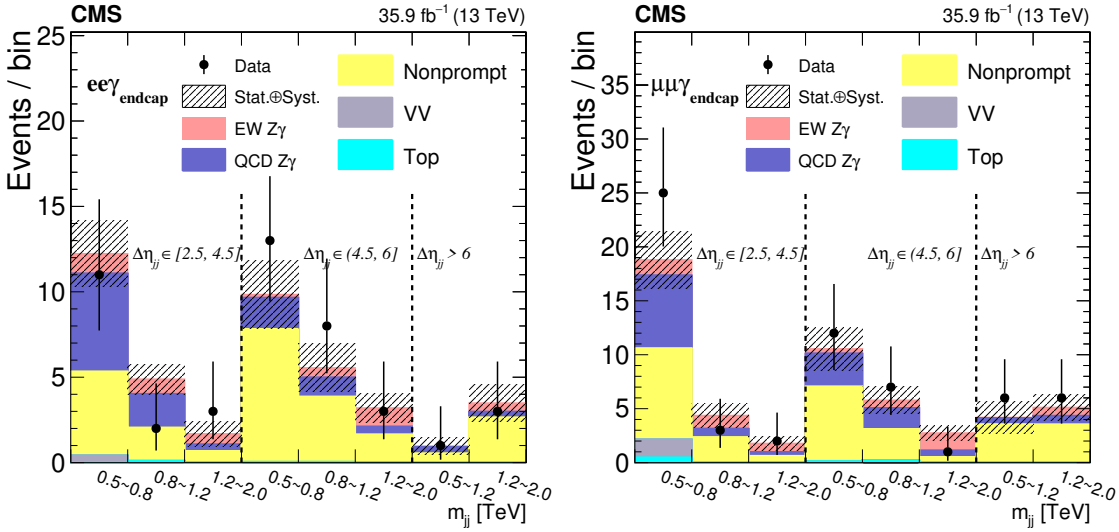

Figure 5. The post-fit 2D distributions of the dielectron (left) and dimuon (right) + γ_{endcap} categories as a function of m_{jj} in bins of $\Delta\eta_{\text{jj}}$. The horizontal axis is split into bins of $\Delta\eta_{\text{jj}}$ of [2.5, 4.5], (4.5, 6.0], and > 6.0. The data are compared to the signal and background predictions in the signal region. The black points with error bars represent the data and statistical uncertainties of data, the hatched bands represent the full uncertainties of the predictions.

JHEP06(2020)076

where σ_g is the cross section for the generated signal events, $\hat{\mu}$ is the signal strength parameter, and a_{gf} is the acceptance for the events generated in the fiducial region and evaluated through simulation. The fiducial cross section for the EW Zγ signal obtained from MadGraph5_aMC@NLO at LO accuracy is $4.97 \pm 0.25(\text{scale}) \pm 0.14(\text{PDF})$ fb. The best fit value for the EW Zγ signal strength is 0.65 ± 0.24 and the measured fiducial cross section is

$$\sigma_{EW}^{fid} = 3.2 \pm 0.2\,(\text{lumi}) \pm 1.1\,(\text{stat}) \pm 0.6\,(\text{syst})\,\text{fb} = 3.2 \pm 1.2\,\text{fb}.$$

A combined Zγjj cross section is measured in the same fiducial region using the same procedure, except that the control region is excluded. The combined Zγjj cross section is defined as

$$\sigma^{fid} = \hat{\mu}\{\sigma_g^{EW} a_{gf}^{EW} + \sigma_g^{QCD} a_{gf}^{QCD}\}.$$

The fiducial cross section for all QCD-induced Zγjj events expected from MadGraph5_aMC @NLO at NLO accuracy is $10.7 \pm 1.7\,(\text{scale}) \pm 0.2\,(\text{PDF})$ fb. The expected fiducial cross section for the combined QCD and EW Zγjj production is $15.7 \pm 1.7\,(\text{scale}) \pm 0.2(\text{PDF})$ fb. The best fit value for the combined Zγjj signal strength is 0.91 ± 0.19, and the measured cross section is

$$\sigma_{EW+QCD}^{fid} = 14.3 \pm 0.4\,(\text{lumi}) \pm 1.1\,(\text{stat}) \pm 2.7\,(\text{syst})\,\text{fb} = 14.3 \pm 3.0\,\text{fb}.$$

7.3 Limits on anomalous quartic gauge couplings

The effects of BSM physics can be modeled in a generic way through a collection of linearly independent higher dimensional operators in effective field theory [6]. Reference [7] proposes nine independent charge-conjugate and parity-conserving dimension-eight effective operators by assuming the SU(2)×U(1) symmetry of the EW gauge field, including a Higgs doublet to incorporate the presence of an SM Higgs boson. A contribution from aQGCs would enhance the production of events with large Zγ mass. The operators affecting the Zγjj channel can be divided into those containing an SU(2) field strength, the U(1) field strength, the covariant derivative of the Higgs doublet, $\mathcal{L}_{M,0} - \mathcal{L}_{M,7}$, and those containing only the two field strengths, $\mathcal{L}_{T,0} - \mathcal{L}_{T,9}$. The coefficient of the operator $\mathcal{L}_{X,Y}$ is denoted by $F_{X,Y}/\Lambda^4$, where Λ is the unknown scale of BSM physics.

A simulation is performed that includes the effects of the aQGCs in addition to the SM EW Zγ process, as well as any interference between the two. We use the $m_{Z\gamma}$ distribution to extract limits on aQGC parameters. To obtain a continuous prediction for the signal as a function of the anomalous coupling, a quadratic fit is performed to the SM+aQGC yield as a function of $m_{Z\gamma}$ bin in the aQGC region defined in section 4.2. From figure 6, no statistically significant excess of events relative to the SM prediction. The following profile likelihood test statistic is used in the aQGC limit setting procedure:

$$t_{\alpha_{test}} = -2 \log \frac{\mathcal{L}(\alpha_{test}, \hat{\hat{\boldsymbol{\theta}}})}{\mathcal{L}(\hat{\alpha}, \hat{\boldsymbol{\theta}})}.$$

JHEP06(2020)076

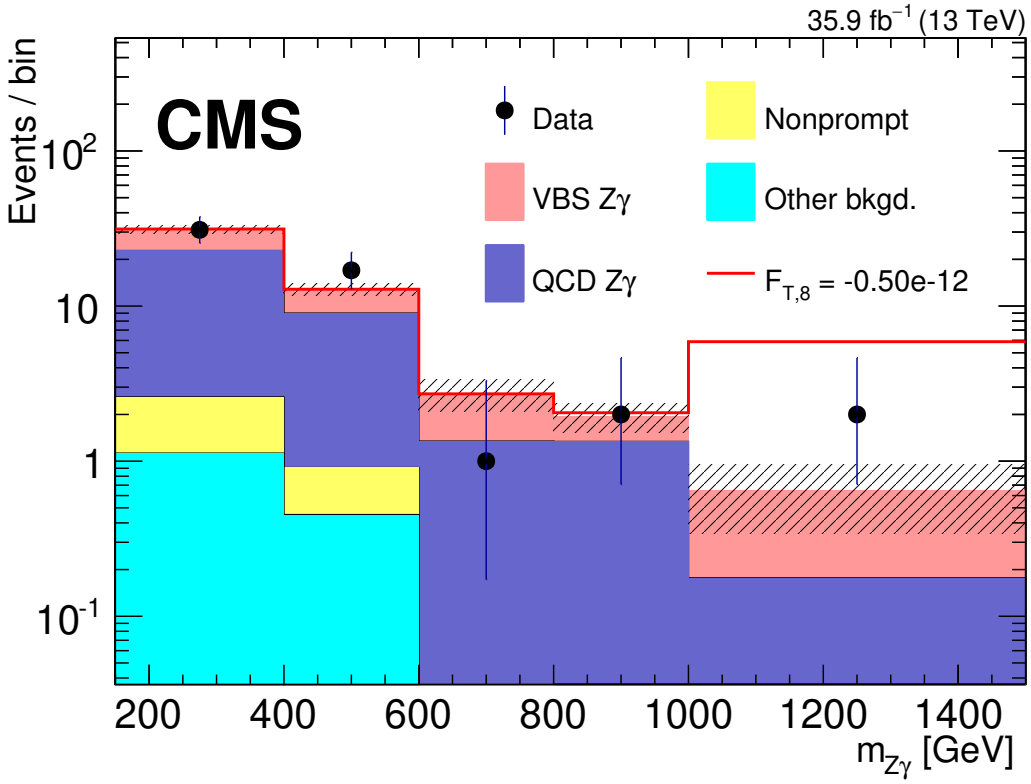

Figure 6. The $m_{Z\gamma}$ distribution of events satisfying the aQGC region selection, which is used to set constraints on the anomalous coupling parameters. The red line represents a nonzero $F_{T,8}$ setting, which would significantly enhance the yields at high $m_{Z\gamma}$. The bins of $m_{Z\gamma}$ are [100, 400, 600, 800, 1000, 1500] GeV, where the last bin includes overflow. The hatched bands represent the statistical uncertainties in the predictions.

The likelihood function is the product of Poisson distributions and a normal constraining term with nuisance parameters representing the sources of systematic uncertainties in any given bin. The final likelihood function is the product of the likelihood functions of the electron and muon channels. The main constraint on aQGCs parameter is from the last bin. The α_{test} represents the aQGC point being tested, and the symbol $\boldsymbol{\theta}$ represents a vector of nuisance parameters assumed to follow log-normal distributions. The parameter $\hat{\hat{\boldsymbol{\theta}}}$ corresponds to the maximum of the likelihood function at the point α_{test}. The $\hat{\alpha}$ and $\hat{\boldsymbol{\theta}}$ parameters correspond to the global maximum of the likelihood function.

This test statistic is assumed to follow a χ^2 distribution [48]. It is therefore possible to extract the limits immediately from the difference in the log-likelihood function $\Delta\text{NLL} = t_{\alpha_{\text{test}}}/2$ [49]. The 95% confidence level (CL) limit on a one dimensional aQGC parameter corresponds to $2\Delta\text{NLL} = 3.84$. Figure 7 shows the likelihood scan of parameter $F_{T,8}$ in the calculation of the observed and expected limits. The observed and expected 95% CL limits for the coefficients, shown in table 4, are obtained by varying the coefficients of one nonzero operator coefficient at a time. The observed limits are less stringent than those expected because of an excess of events at large $m_{Z\gamma}$, where you would expect aQGC signal, at approximately one standard deviation level. The unitarity bound is defined

JHEP06(2020)076

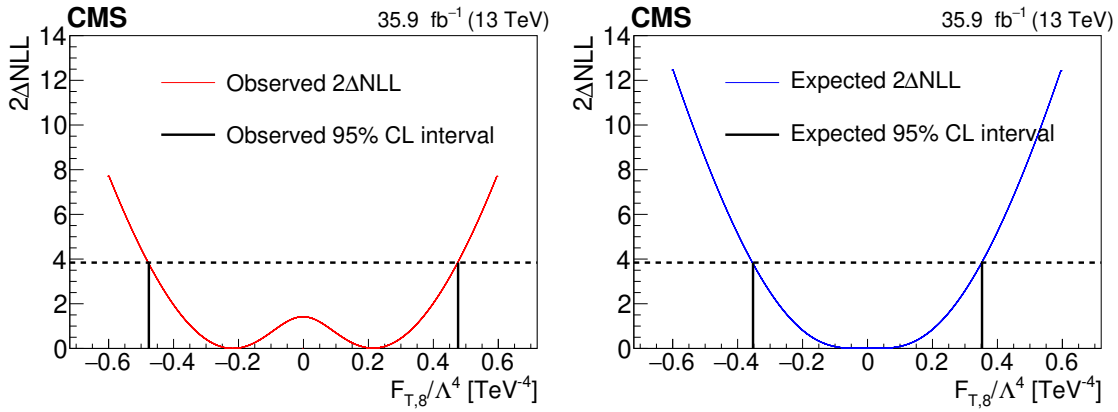

Figure 7. Observed (left) and expected (right) 95% CL intervals on the aQGC parameter $F_{\mathrm{T},8}$.

Observed limits [TeV $^{-4}$]	Expected limits [TeV $^{-4}$]	Unitarity bound [TeV]
$-19.5 < F_{\mathrm{M},0}/\Lambda^4 < 20.3$	$-15.0 < F_{\mathrm{M},0}/\Lambda^4 < 15.0$	1.0
$-40.5 < F_{\mathrm{M},1}/\Lambda^4 < 39.5$	$-30.0 < F_{\mathrm{M},1}/\Lambda^4 < 29.9$	1.2
$-8.22 < F_{\mathrm{M},2}/\Lambda^4 < 8.10$	$-6.09 < F_{\mathrm{M},2}/\Lambda^4 < 6.06$	1.3
$-17.7 < F_{\mathrm{M},3}/\Lambda^4 < 17.9$	$-13.1 < F_{\mathrm{M},3}/\Lambda^4 < 13.2$	1.4
$-15.3 < F_{\mathrm{M},4}/\Lambda^4 < 15.8$	$-11.7 < F_{\mathrm{M},4}/\Lambda^4 < 11.7$	1.4
$-25.1 < F_{\mathrm{M},5}/\Lambda^4 < 24.5$	$-19.0 < F_{\mathrm{M},5}/\Lambda^4 < 18.1$	1.8
$-38.9 < F_{\mathrm{M},6}/\Lambda^4 < 40.6$	$-29.9 < F_{\mathrm{M},6}/\Lambda^4 < 30.0$	1.0
$-60.3 < F_{\mathrm{M},7}/\Lambda^4 < 62.5$	$-45.9 < F_{\mathrm{M},7}/\Lambda^4 < 46.1$	1.3
$-0.74 < F_{\mathrm{T},0}/\Lambda^4 < 0.69$	$-0.56 < F_{\mathrm{T},0}/\Lambda^4 < 0.51$	1.4
$-0.98 < F_{\mathrm{T},1}/\Lambda^4 < 0.96$	$-0.72 < F_{\mathrm{T},1}/\Lambda^4 < 0.72$	1.4
$-1.97 < F_{\mathrm{T},2}/\Lambda^4 < 1.86$	$-1.47 < F_{\mathrm{T},2}/\Lambda^4 < 1.37$	1.4
$-0.70 < F_{\mathrm{T},5}/\Lambda^4 < 0.75$	$-0.51 < F_{\mathrm{T},5}/\Lambda^4 < 0.57$	1.7
$-1.64 < F_{\mathrm{T},6}/\Lambda^4 < 1.68$	$-1.23 < F_{\mathrm{T},6}/\Lambda^4 < 1.26$	1.6
$-2.59 < F_{\mathrm{T},7}/\Lambda^4 < 2.82$	$-1.91 < F_{\mathrm{T},7}/\Lambda^4 < 2.12$	1.7
$-0.47 < F_{\mathrm{T},8}/\Lambda^4 < 0.47$	$-0.36 < F_{\mathrm{T},8}/\Lambda^4 < 0.36$	1.5
$-1.27 < F_{\mathrm{T},9}/\Lambda^4 < 1.27$	$-0.94 < F_{\mathrm{T},9}/\Lambda^4 < 0.94$	1.5

Table 4. 95% CL exclusion limits in units of TeV $^{-4}$; the unitarity bounds are also listed in units of TeV.

as the scattering energy at which the aQGC coupling strength set equal to the observed limit would result in a scattering amplitude that violates unitarity. The value of the unitarity bound is determined using the VBFNLO 2.7.1 framework [50], taking into account the difference between VBFNLO and MadGraph5_aMC@NLO. These results provide the most stringent limits to date on the aQGC parameters $F_{\mathrm{T},8}/\Lambda^4$ and $F_{\mathrm{T},9}/\Lambda^4$.

JHEP06(2020)076

8 Summary

A new measurement has been made of vector boson scattering in the $\mathrm{Z}\gamma\mathrm{jj}$ channel. The data, collected in proton-proton collisions at $\sqrt{s} = 13\,\mathrm{TeV}$ in the CMS detector in 2016, correspond to an integrated luminosity of $35.9\,\mathrm{fb}^{-1}$. Events were selected by requiring two identified oppositely charged electrons or muons with invariant mass consistent with a Z boson, one identified photon, and two jets that have a large separation in pseudorapidity and a large dijet mass. The observed significance for a signal in the data is 3.9 standard deviations (s.d.), where a significance of 5.2 s.d. is expected based on the standard model. When this result is combined with previous CMS measurements at 8 TeV, the observed and expected significances become respectively 4.7 and 5.5 s.d. The fiducial cross section for electroweak $\mathrm{Z}\gamma\mathrm{jj}$ production is $3.2 \pm 1.2\,\mathrm{fb}$ for the data at 13 TeV, and the fiducial cross section for the sum of sources from electroweak and from quantum chromodynamics is $14.3 \pm 3.0\,\mathrm{fb}$. Constraints placed on anomalous quartic gauge couplings in terms of dimension-eight operators in effective field theory are either competitive with or more stringent than those previously obtained.

Acknowledgments

We congratulate our colleagues in the CERN accelerator departments for the excellent performance of the LHC and thank the technical and administrative staffs at CERN and at other CMS institutes for their contributions to the success of the CMS effort. In addition, we gratefully acknowledge the computing centers and personnel of the Worldwide LHC Computing Grid for delivering so effectively the computing infrastructure essential to our analyses. Finally, we acknowledge the enduring support for the construction and operation of the LHC and the CMS detector provided by the following funding agencies: BMBWF and FWF (Austria); FNRS and FWO (Belgium); CNPq, CAPES, FAPERJ, FAPERGS, and FAPESP (Brazil); MES (Bulgaria); CERN; CAS, MoST, and NSFC (China); COLCIENCIAS (Colombia); MSES and CSF (Croatia); RPF (Cyprus); SENESCYT (Ecuador); MoER, ERC IUT, PUT and ERDF (Estonia); Academy of Finland, MEC, and HIP (Finland); CEA and CNRS/IN2P3 (France); BMBF, DFG, and HGF (Germany); GSRT (Greece); NKFIA (Hungary); DAE and DST (India); IPM (Iran); SFI (Ireland); INFN (Italy); MSIP and NRF (Republic of Korea); MES (Latvia); LAS (Lithuania); MOE and UM (Malaysia); BUAP, CINVESTAV, CONACYT, LNS, SEP, and UASLP-FAI (Mexico); MOS (Montenegro); MBIE (New Zealand); PAEC (Pakistan); MSHE and NSC (Poland); FCT (Portugal); JINR (Dubna); MON, RosAtom, RAS, RFBR, and NRC KI (Russia); MESTD (Serbia); SEIDI, CPAN, PCTI, and FEDER (Spain); MOSTR (Sri Lanka); Swiss Funding Agencies (Switzerland); MST (Taipei); ThEPCenter, IPST, STAR, and NSTDA (Thailand); TUBITAK and TAEK (Turkey); NASU (Ukraine); STFC (United Kingdom); DOE and NSF (U.S.A.).

Individuals have received support from the Marie-Curie program and the European Research Council and Horizon 2020 Grant, contract Nos. 675440, 752730, and 765710 (European Union); the Leventis Foundation; the A.P. Sloan Foundation; the Alexander von

JHEP06(2020)076

Humboldt Foundation; the Belgian Federal Science Policy Office; the Fonds pour la Formation à la Recherche dans l'Industrie et dans l'Agriculture (FRIA-Belgium); the Agentschap voor Innovatie door Wetenschap en Technologie (IWT-Belgium); the F.R.S.-FNRS and FWO (Belgium) under the "Excellence of Science — EOS" — be.h project n. 30820817; the Beijing Municipal Science & Technology Commission, No. Z191100007219010; the Ministry of Education, Youth and Sports (MEYS) of the Czech Republic; the Deutsche Forschungsgemeinschaft (DFG) under Germany's Excellence Strategy — EXC 2121 "Quantum Universe" — 390833306; the Lendület ("Momentum") Program and the János Bolyai Research Scholarship of the Hungarian Academy of Sciences, the New National Excellence Program ÚNKP, the NKFIA research grants 123842, 123959, 124845, 124850, 125105, 128713, 128786, and 129058 (Hungary); the Council of Science and Industrial Research, India; the HOMING PLUS program of the Foundation for Polish Science, cofinanced from European Union, Regional Development Fund, the Mobility Plus program of the Ministry of Science and Higher Education, the National Science Center (Poland), contracts Harmonia 2014/14/M/ST2/00428, Opus 2014/13/B/ST2/02543, 2014/15/B/ST2/03998, and 2015/19/B/ST2/02861, Sonata-bis 2012/07/E/ST2/01406; the National Priorities Research Program by Qatar National Research Fund; the Ministry of Science and Education, grant no. 14.W03.31.0026 (Russia); the Tomsk Polytechnic University Competitiveness Enhancement Program and "Nauka" Project FSWW-2020-0008 (Russia); the Programa Estatal de Fomento de la Investigación Científica y Técnica de Excelencia María de Maeztu, grant MDM-2015-0509 and the Programa Severo Ochoa del Principado de Asturias; the Thalis and Aristeia programs cofinanced by EU-ESF and the Greek NSRF; the Rachadapisek Sompot Fund for Postdoctoral Fellowship, Chulalongkorn University and the Chulalongkorn Academic into Its 2nd Century Project Advancement Project (Thailand); the Kavli Foundation; the Nvidia Corporation; the SuperMicro Corporation; the Welch Foundation, contract C-1845; and the Weston Havens Foundation (U.S.A.).

JHEP06(2020)076

References

[1] ATLAS collaboration, *Observation of a new particle in the search for the Standard Model Higgs boson with the ATLAS detector at the LHC*, *Phys. Lett.* **B 716** (2012) 1 [arXiv:1207.7214] [INSPIRE].

[2] CMS collaboration, *Observation of a New Boson at a Mass of* 125 *GeV with the CMS Experiment at the LHC*, *Phys. Lett.* **B 716** (2012) 30 [arXiv:1207.7235] [INSPIRE].

[3] CMS collaboration, *Observation of a New Boson with Mass Near* 125 *GeV in pp Collisions at* $\sqrt{s} = 7$ *and* 8 *TeV*, *JHEP* **06** (2013) 081 [arXiv:1303.4571] [INSPIRE].

[4] ATLAS and CMS collaborations, *Measurements of the Higgs boson production and decay rates and constraints on its couplings from a combined ATLAS and CMS analysis of the LHC pp collision data at* $\sqrt{s} = 7$ *and* 8 *TeV*, *JHEP* **08** (2016) 045 [arXiv:1606.02266] [INSPIRE].

[5] CMS collaboration, *Combined measurements of Higgs boson couplings in proton-proton collisions at* $\sqrt{s} = 13$ *TeV*, *Eur. Phys. J.* **C 79** (2019) 421 [arXiv:1809.10733] [INSPIRE].

[6] C. Degrande et al., *Effective Field Theory: A Modern Approach to Anomalous Couplings*, *Annals Phys.* **335** (2013) 21 [arXiv:1205.4231] [INSPIRE].

[7] O.J.P. Éboli, M.C. Gonzalez-Garcia and J.K. Mizukoshi, $pp \to jje^{\pm}\mu^{\pm}\nu\nu$ *and* $jje^{\pm}\mu^{\mp}\nu\nu$ *at* $\mathcal{O}(\alpha_{\rm em}^6)$ *and* $\mathcal{O}(\alpha_{\rm em}^4\alpha_s^2)$ *for the study of the quartic electroweak gauge boson vertex at CERN LHC*, *Phys. Rev.* **D 74** (2006) 073005 [hep-ph/0606118] [INSPIRE].

[8] ATLAS collaboration, *Observation of electroweak production of a same-sign W boson pair in association with two jets in pp collisions at* $\sqrt{s} = 13$ *TeV with the ATLAS detector*, *Phys. Rev. Lett.* **123** (2019) 161801 [arXiv:1906.03203] [INSPIRE].

[9] CMS collaboration, *Observation of electroweak production of same-sign W boson pairs in the two jet and two same-sign lepton final state in proton-proton collisions at* $\sqrt{s} = 13$ *TeV*, *Phys. Rev. Lett.* **120** (2018) 081801 [arXiv:1709.05822] [INSPIRE].

[10] ATLAS collaboration, *Observation of electroweak* $W^{\pm}Z$ *boson pair production in association with two jets in pp collisions at* $\sqrt{s} = 13$ *TeV with the ATLAS detector*, *Phys. Lett.* **B 793** (2019) 469 [arXiv:1812.09740] [INSPIRE].

[11] ATLAS collaboration, *Studies of* $Z\gamma$ *production in association with a high-mass dijet system in pp collisions at* $\sqrt{s} = 8$ *TeV with the ATLAS detector*, *JHEP* **07** (2017) 107 [arXiv:1705.01966] [INSPIRE].

[12] CMS collaboration, *Measurement of the cross section for electroweak production of* $Z\gamma$ *in association with two jets and constraints on anomalous quartic gauge couplings in proton-proton collisions at* $\sqrt{s} = 8$ *TeV*, *Phys. Lett.* **B 770** (2017) 380 [arXiv:1702.03025] [INSPIRE].

[13] ATLAS collaboration, *Evidence for electroweak production of two jets in association with a* $Z\gamma$ *pair in pp collisions at* $\sqrt{s} = 13$ *TeV with the ATLAS detector*, *Phys. Lett.* **B 803** (2020) 135341 [arXiv:1910.09503] [INSPIRE].

[14] CMS collaboration, *The CMS Experiment at the CERN LHC*, 2008 *JINST* **3** S08004 [INSPIRE].

[15] CMS collaboration, *The CMS trigger system*, 2017 *JINST* **12** P01020 [arXiv:1609.02366] [INSPIRE].

[16] J. Alwall et al., *The automated computation of tree-level and next-to-leading order differential cross sections and their matching to parton shower simulations*, *JHEP* **07** (2014) 079 [arXiv:1405.0301] [INSPIRE].

[17] R. Frederix and S. Frixione, *Merging meets matching in MC@NLO*, *JHEP* **12** (2012) 061 [arXiv:1209.6215] [INSPIRE].

[18] T. Sjöstrand et al., *An Introduction to PYTHIA 8.2*, *Comput. Phys. Commun.* **191** (2015) 159 [arXiv:1410.3012] [INSPIRE].

[19] T. Melia, P. Nason, R. Rontsch and G. Zanderighi, W^+W^-, *WZ and ZZ production in the POWHEG BOX*, *JHEP* **11** (2011) 078 [arXiv:1107.5051] [INSPIRE].

[20] P. Nason, *A New method for combining NLO QCD with shower Monte Carlo algorithms*, *JHEP* **11** (2004) 040 [hep-ph/0409146] [INSPIRE].

JHEP06(2020)076

[21] S. Frixione, P. Nason and C. Oleari, *Matching NLO QCD computations with Parton Shower simulations: the POWHEG method*, *JHEP* **11** (2007) 070 [arXiv:0709.2092] [INSPIRE].

[22] S. Alioli, P. Nason, C. Oleari and E. Re, *A general framework for implementing NLO calculations in shower Monte Carlo programs: the POWHEG BOX*, *JHEP* **06** (2010) 043 [arXiv:1002.2581] [INSPIRE].

[23] O. Mattelaer, *On the maximal use of Monte Carlo samples: re-weighting events at NLO accuracy*, *Eur. Phys. J.* **C 76** (2016) 674 [arXiv:1607.00763] [INSPIRE].

[24] P. Skands, S. Carrazza and J. Rojo, *Tuning PYTHIA 8.1: the Monash 2013 Tune*, *Eur. Phys. J.* **C 74** (2014) 3024 [arXiv:1404.5630] [INSPIRE].

[25] CMS collaboration, *Event generator tunes obtained from underlying event and multiparton scattering measurements*, *Eur. Phys. J.* **C 76** (2016) 155 [arXiv:1512.00815] [INSPIRE].

[26] NNPDF collaboration, *Parton distributions for the LHC Run II*, *JHEP* **04** (2015) 040 [arXiv:1410.8849] [INSPIRE].

[27] GEANT4 collaboration, *GEANT4: A Simulation toolkit*, *Nucl. Instrum. Meth.* **A 506** (2003) 250 [INSPIRE].

[28] J. Allison et al., *Geant4 developments and applications*, *IEEE Trans. Nucl. Sci.* **53** (2006) 270 [INSPIRE].

[29] CMS collaboration, *Measurement of the Inclusive W and Z Production Cross Sections in pp Collisions at* $\sqrt{s} = 7$ *TeV*, *JHEP* **10** (2011) 132 [arXiv:1107.4789] [INSPIRE].

[30] CMS collaboration, *Particle-flow reconstruction and global event description with the CMS detector*, 2017 *JINST* **12** P10003 [arXiv:1706.04965] [INSPIRE].

[31] CMS collaboration, *Description and performance of track and primary-vertex reconstruction with the CMS tracker*, 2014 *JINST* **9** P10009 [arXiv:1405.6569] [INSPIRE].

[32] M. Cacciari, G.P. Salam and G. Soyez, *The anti-k_t jet clustering algorithm*, *JHEP* **04** (2008) 063 [arXiv:0802.1189] [INSPIRE].

[33] M. Cacciari, G.P. Salam and G. Soyez, *FastJet User Manual*, *Eur. Phys. J.* **C 72** (2012) 1896 [arXiv:1111.6097] [INSPIRE].

[34] CMS collaboration, *Performance of Electron Reconstruction and Selection with the CMS Detector in Proton-Proton Collisions at* $\sqrt{s} = 8$ *TeV*, 2015 *JINST* **10** P06005 [arXiv:1502.02701] [INSPIRE].

[35] CMS collaboration, *Energy Calibration and Resolution of the CMS Electromagnetic Calorimeter in pp Collisions at* $\sqrt{s} = 7$ *TeV*, 2013 *JINST* **8** P09009 [arXiv:1306.2016] [INSPIRE].

[36] CMS collaboration, *Performance of the CMS muon detector and muon reconstruction with proton-proton collisions at* $\sqrt{s} = 13$ *TeV*, 2018 *JINST* **13** P06015 [arXiv:1804.04528] [INSPIRE].

[37] M. Cacciari and G.P. Salam, *Pileup subtraction using jet areas*, *Phys. Lett.* **B 659** (2008) 119 [arXiv:0707.1378] [INSPIRE].

[38] CMS collaboration, *Performance of Photon Reconstruction and Identification with the CMS Detector in Proton-Proton Collisions at* $\sqrt{s} = 8$ *TeV*, 2015 *JINST* **10** P08010 [arXiv:1502.02702] [INSPIRE].

JHEP06(2020)076

[39] CMS collaboration, *Jet energy scale and resolution in the CMS experiment in pp collisions at 8 TeV*, 2017 *JINST* **12** P02014 [arXiv:1607.03663] [INSPIRE].

[40] D.L. Rainwater, R. Szalapski and D. Zeppenfeld, *Probing color singlet exchange in Z + two jet events at the CERN LHC*, *Phys. Rev.* **D 54** (1996) 6680 [hep-ph/9605444] [INSPIRE].

[41] CMS collaboration, *Measurement of $W\gamma$ and $Z\gamma$ production in pp collisions at $\sqrt{s} = 7$ TeV*, *Phys. Lett.* **B 701** (2011) 535 [arXiv:1105.2758] [INSPIRE].

[42] N. Kidonakis, *Two-loop soft anomalous dimensions for single top quark associated production with a W^- or H^-*, *Phys. Rev.* **D 82** (2010) 054018 [arXiv:1005.4451] [INSPIRE].

[43] CMS collaboration, *CMS Luminosity Measurements for the 2016 Data Taking Period*, CMS-PAS-LUM-17-001 (2017) [INSPIRE].

[44] J. Butterworth et al., *PDF4LHC recommendations for LHC Run II*, *J. Phys.* **G 43** (2016) 023001 [arXiv:1510.03865] [INSPIRE].

[45] T. Junk, *Confidence level computation for combining searches with small statistics*, *Nucl. Instrum. Meth.* **A 434** (1999) 435 [hep-ex/9902006] [INSPIRE].

[46] A.L. Read, *Presentation of search results: The CL_s technique*, *J. Phys.* **G 28** (2002) 2693 [INSPIRE].

[47] G. Cowan, K. Cranmer, E. Gross and O. Vitells, *Asymptotic formulae for likelihood-based tests of new physics*, *Eur. Phys. J.* **C 71** (2011) 1554 [*Erratum ibid.* **C 73** (2013) 2501] [arXiv:1007.1727] [INSPIRE].

[48] S.S. Wilks, *The large-sample distribution of the likelihood ratio for testing composite hypotheses*, *Ann. Math. Stat.* **9** (1938) 60 [INSPIRE].

[49] CMS collaboration, *Precise determination of the mass of the Higgs boson and tests of compatibility of its couplings with the standard model predictions using proton collisions at 7 and 8 TeV*, *Eur. Phys. J.* **C 75** (2015) 212 [arXiv:1412.8662] [INSPIRE].

[50] K. Arnold et al., *VBFNLO: A Parton level Monte Carlo for processes with electroweak bosons*, *Comput. Phys. Commun.* **180** (2009) 1661 [arXiv:0811.4559] [INSPIRE].

JHEP06(2020)076

The CMS collaboration

Yerevan Physics Institute, Yerevan, Armenia

A.M. Sirunyan[†], A. Tumasyan

Institut für Hochenergiephysik, Wien, Austria

W. Adam, F. Ambrogi, T. Bergauer, J. Brandstetter, M. Dragicevic, J. Erö, A. Escalante Del Valle, M. Flechl, R. Frühwirth[1], M. Jeitler[1], N. Krammer, I. Krätschmer, D. Liko, T. Madlener, I. Mikulec, N. Rad, J. Schieck[1], R. Schöfbeck, M. Spanring, D. Spitzbart, W. Waltenberger, C.-E. Wulz[1], M. Zarucki

Institute for Nuclear Problems, Minsk, Belarus

V. Drugakov, V. Mossolov, J. Suarez Gonzalez

Universiteit Antwerpen, Antwerpen, Belgium

M.R. Darwish, E.A. De Wolf, D. Di Croce, X. Janssen, A. Lelek, M. Pieters, H. Rejeb Sfar, H. Van Haevermaet, P. Van Mechelen, S. Van Putte, N. Van Remortel

Vrije Universiteit Brussel, Brussel, Belgium

F. Blekman, E.S. Bols, S.S. Chhibra, J. D'Hondt, J. De Clercq, D. Lontkovskyi, S. Lowette, I. Marchesini, S. Moortgat, Q. Python, K. Skovpen, S. Tavernier, W. Van Doninck, P. Van Mulders

Université Libre de Bruxelles, Bruxelles, Belgium

D. Beghin, B. Bilin, H. Brun, B. Clerbaux, G. De Lentdecker, H. Delannoy, B. Dorney, L. Favart, A. Grebenyuk, A.K. Kalsi, A. Popov, N. Postiau, E. Starling, L. Thomas, C. Vander Velde, P. Vanlaer, D. Vannerom

Ghent University, Ghent, Belgium

T. Cornelis, D. Dobur, I. Khvastunov[2], M. Niedziela, C. Roskas, D. Trocino, M. Tytgat, W. Verbeke, B. Vermassen, M. Vit

Université Catholique de Louvain, Louvain-la-Neuve, Belgium

O. Bondu, G. Bruno, C. Caputo, P. David, C. Delaere, M. Delcourt, A. Giammanco, V. Lemaitre, J. Prisciandaro, A. Saggio, M. Vidal Marono, P. Vischia, J. Zobec

Centro Brasileiro de Pesquisas Fisicas, Rio de Janeiro, Brazil

F.L. Alves, G.A. Alves, G. Correia Silva, C. Hensel, A. Moraes, P. Rebello Teles

Universidade do Estado do Rio de Janeiro, Rio de Janeiro, Brazil

E. Belchior Batista Das Chagas, W. Carvalho, J. Chinellato[3], E. Coelho, E.M. Da Costa, G.G. Da Silveira[4], D. De Jesus Damiao, C. De Oliveira Martins, S. Fonseca De Souza, L.M. Huertas Guativa, H. Malbouisson, J. Martins[5], D. Matos Figueiredo, M. Medina Jaime[6], M. Melo De Almeida, C. Mora Herrera, L. Mundim, H. Nogima, W.L. Prado Da Silva, L.J. Sanchez Rosas, A. Santoro, A. Sznajder, M. Thiel, E.J. Tonelli Manganote[3], F. Torres Da Silva De Araujo, A. Vilela Pereira

JHEP06(2020)076

Universidade Estadual Paulista[a], Universidade Federal do ABC[b], São Paulo, Brazil

C.A. Bernardes[a], L. Calligaris[a], T.R. Fernandez Perez Tomei[a], E.M. Gregores[b], D.S. Lemos, P.G. Mercadante[b], S.F. Novaes[a], SandraS. Padula[a]

Institute for Nuclear Research and Nuclear Energy, Bulgarian Academy of Sciences, Sofia, Bulgaria

A. Aleksandrov, G. Antchev, R. Hadjiiska, P. Iaydjiev, M. Misheva, M. Rodozov, M. Shopova, G. Sultanov

University of Sofia, Sofia, Bulgaria

M. Bonchev, A. Dimitrov, T. Ivanov, L. Litov, B. Pavlov, P. Petkov

Beihang University, Beijing, China

W. Fang[7], X. Gao[7], L. Yuan

Department of Physics, Tsinghua University, Beijing, China

M. Ahmad, Z. Hu, Y. Wang

Institute of High Energy Physics, Beijing, China

G.M. Chen, H.S. Chen, M. Chen, C.H. Jiang, D. Leggat, H. Liao, Z. Liu, A. Spiezia, J. Tao, E. Yazgan, H. Zhang, S. Zhang[8], J. Zhao

State Key Laboratory of Nuclear Physics and Technology, Peking University, Beijing, China

A. Agapitos, Y. Ban, G. Chen, A. Levin, J. Li, L. Li, Q. Li, M. Lu, Y. Mao, S.J. Qian, D. Wang, Q. Wang

Zhejiang University, Hangzhou, China

M. Xiao

Universidad de Los Andes, Bogota, Colombia

C. Avila, A. Cabrera, C. Florez, C.F. González Hernández, M.A. Segura Delgado

Universidad de Antioquia, Medellin, Colombia

J. Mejia Guisao, J.D. Ruiz Alvarez, C.A. Salazar González, N. Vanegas Arbelaez

University of Split, Faculty of Electrical Engineering, Mechanical Engineering and Naval Architecture, Split, Croatia

D. Giljanović, N. Godinovic, D. Lelas, I. Puljak, T. Sculac

University of Split, Faculty of Science, Split, Croatia

Z. Antunovic, M. Kovac

Institute Rudjer Boskovic, Zagreb, Croatia

V. Brigljevic, D. Ferencek, K. Kadija, B. Mesic, M. Roguljic, A. Starodumov[9], T. Susa

University of Cyprus, Nicosia, Cyprus

M.W. Ather, A. Attikis, E. Erodotou, A. Ioannou, M. Kolosova, S. Konstantinou, G. Mavromanolakis, J. Mousa, C. Nicolaou, F. Ptochos, P.A. Razis, H. Rykaczewski, D. Tsiakkouri

JHEP06(2020)076

Charles University, Prague, Czech Republic
M. Finger[10], M. Finger Jr.[10], A. Kveton, J. Tomsa

Escuela Politecnica Nacional, Quito, Ecuador
E. Ayala

Universidad San Francisco de Quito, Quito, Ecuador
E. Carrera Jarrin

Academy of Scientific Research and Technology of the Arab Republic of Egypt, Egyptian Network of High Energy Physics, Cairo, Egypt
Y. Assran[11,12], S. Elgammal[12]

National Institute of Chemical Physics and Biophysics, Tallinn, Estonia
S. Bhowmik, A. Carvalho Antunes De Oliveira, R.K. Dewanjee, K. Ehataht, M. Kadastik, M. Raidal, C. Veelken

Department of Physics, University of Helsinki, Helsinki, Finland
P. Eerola, L. Forthomme, H. Kirschenmann, K. Osterberg, M. Voutilainen

Helsinki Institute of Physics, Helsinki, Finland
F. Garcia, J. Havukainen, J.K. Heikkilä, V. Karimäki, M.S. Kim, R. Kinnunen, T. Lampén, K. Lassila-Perini, S. Laurila, S. Lehti, T. Lindén, P. Luukka, T. Mäenpää, H. Siikonen, E. Tuominen, J. Tuominiemi

Lappeenranta University of Technology, Lappeenranta, Finland
T. Tuuva

IRFU, CEA, Université Paris-Saclay, Gif-sur-Yvette, France
M. Besancon, F. Couderc, M. Dejardin, D. Denegri, B. Fabbro, J.L. Faure, F. Ferri, S. Ganjour, A. Givernaud, P. Gras, G. Hamel de Monchenault, P. Jarry, C. Leloup, E. Locci, J. Malcles, J. Rander, A. Rosowsky, M.Ö. Sahin, A. Savoy-Navarro[13], M. Titov

Laboratoire Leprince-Ringuet, CNRS/IN2P3, Ecole Polytechnique, Institut Polytechnique de Paris
S. Ahuja, C. Amendola, F. Beaudette, P. Busson, C. Charlot, B. Diab, G. Falmagne, R. Granier de Cassagnac, I. Kucher, A. Lobanov, C. Martin Perez, M. Nguyen, C. Ochando, P. Paganini, J. Rembser, R. Salerno, J.B. Sauvan, Y. Sirois, A. Zabi, A. Zghiche

Université de Strasbourg, CNRS, IPHC UMR 7178, Strasbourg, France
J.-L. Agram[14], J. Andrea, D. Bloch, G. Bourgatte, J.-M. Brom, E.C. Chabert, C. Collard, E. Conte[14], J.-C. Fontaine[14], D. Gelé, U. Goerlach, M. Jansová, A.-C. Le Bihan, N. Tonon, P. Van Hove

Centre de Calcul de l'Institut National de Physique Nucleaire et de Physique des Particules, CNRS/IN2P3, Villeurbanne, France
S. Gadrat

JHEP06(2020)076

Université de Lyon, Université Claude Bernard Lyon 1, CNRS-IN2P3, Institut de Physique Nucléaire de Lyon, Villeurbanne, France

S. Beauceron, C. Bernet, G. Boudoul, C. Camen, A. Carle, N. Chanon, R. Chierici, D. Contardo, P. Depasse, H. El Mamouni, J. Fay, S. Gascon, M. Gouzevitch, B. Ille, Sa. Jain, F. Lagarde, I.B. Laktineh, H. Lattaud, A. Lesauvage, M. Lethuillier, L. Mirabito, S. Perries, V. Sordini, L. Torterotot, G. Touquet, M. Vander Donckt, S. Viret

Georgian Technical University, Tbilisi, Georgia

T. Toriashvili[15]

Tbilisi State University, Tbilisi, Georgia

I. Bagaturia[16]

RWTH Aachen University, I. Physikalisches Institut, Aachen, Germany

C. Autermann, L. Feld, M.K. Kiesel, K. Klein, M. Lipinski, D. Meuser, A. Pauls, M. Preuten, M.P. Rauch, J. Schulz, M. Teroerde, B. Wittmer

RWTH Aachen University, III. Physikalisches Institut A, Aachen, Germany

M. Erdmann, B. Fischer, S. Ghosh, T. Hebbeker, K. Hoepfner, H. Keller, L. Mastrolorenzo, M. Merschmeyer, A. Meyer, P. Millet, G. Mocellin, S. Mondal, S. Mukherjee, D. Noll, A. Novak, T. Pook, A. Pozdnyakov, T. Quast, M. Radziej, Y. Rath, H. Reithler, J. Roemer, A. Schmidt, S.C. Schuler, A. Sharma, S. Wiedenbeck, S. Zaleski

RWTH Aachen University, III. Physikalisches Institut B, Aachen, Germany

G. Flügge, W. Haj Ahmad[17], O. Hlushchenko, T. Kress, T. Müller, A. Nowack, C. Pistone, O. Pooth, D. Roy, H. Sert, A. Stahl[18]

Deutsches Elektronen-Synchrotron, Hamburg, Germany

M. Aldaya Martin, P. Asmuss, I. Babounikau, H. Bakhshiansohi, K. Beernaert, O. Behnke, A. Bermúdez Martínez, D. Bertsche, A.A. Bin Anuar, K. Borras[19], V. Botta, A. Campbell, A. Cardini, P. Connor, S. Consuegra Rodríguez, C. Contreras-Campana, V. Danilov, A. De Wit, M.M. Defranchis, C. Diez Pardos, D. Domínguez Damiani, G. Eckerlin, D. Eckstein, T. Eichhorn, A. Elwood, E. Eren, E. Gallo[20], A. Geiser, A. Grohsjean, M. Guthoff, M. Haranko, A. Harb, A. Jafari, N.Z. Jomhari, H. Jung, A. Kasem[19], M. Kasemann, H. Kaveh, J. Keaveney, C. Kleinwort, J. Knolle, D. Krücker, W. Lange, T. Lenz, J. Lidrych, K. Lipka, W. Lohmann[21], R. Mankel, I.-A. Melzer-Pellmann, A.B. Meyer, M. Meyer, M. Missiroli, G. Mittag, J. Mnich, A. Mussgiller, V. Myronenko, D. Pérez Adán, S.K. Pflitsch, D. Pitzl, A. Raspereza, A. Saibel, M. Savitskyi, V. Scheurer, P. Schütze, C. Schwanenberger, R. Shevchenko, A. Singh, H. Tholen, O. Turkot, A. Vagnerini, M. Van De Klundert, R. Walsh, Y. Wen, K. Wichmann, C. Wissing, O. Zenaiev, R. Zlebcik

University of Hamburg, Hamburg, Germany

R. Aggleton, S. Bein, L. Benato, A. Benecke, V. Blobel, T. Dreyer, A. Ebrahimi, F. Feindt, A. Fröhlich, C. Garbers, E. Garutti, D. Gonzalez, P. Gunnellini, J. Haller, A. Hinzmann, A. Karavdina, G. Kasieczka, R. Klanner, R. Kogler, N. Kovalchuk, S. Kurz, V. Kutzner, J. Lange, T. Lange, A. Malara, J. Multhaup, C.E.N. Niemeyer, A. Perieanu, A. Reimers,

JHEP06(2020)076

O. Rieger, C. Scharf, P. Schleper, S. Schumann, J. Schwandt, J. Sonneveld, H. Stadie, G. Steinbrück, F.M. Stober, B. Vormwald, I. Zoi

Karlsruher Institut fuer Technologie, Karlsruhe, Germany

M. Akbiyik, C. Barth, M. Baselga, S. Baur, T. Berger, E. Butz, R. Caspart, T. Chwalek, W. De Boer, A. Dierlamm, K. El Morabit, N. Faltermann, M. Giffels, P. Goldenzweig, A. Gottmann, M.A. Harrendorf, F. Hartmann[18], U. Husemann, S. Kudella, S. Mitra, M.U. Mozer, D. Müller, Th. Müller, M. Musich, A. Nürnberg, G. Quast, K. Rabbertz, M. Schröder, I. Shvetsov, H.J. Simonis, R. Ulrich, M. Wassmer, M. Weber, C. Wöhrmann, R. Wolf

Institute of Nuclear and Particle Physics (INPP), NCSR Demokritos, Aghia Paraskevi, Greece

G. Anagnostou, P. Asenov, G. Daskalakis, T. Geralis, A. Kyriakis, D. Loukas, G. Paspalaki

National and Kapodistrian University of Athens, Athens, Greece

M. Diamantopoulou, G. Karathanasis, P. Kontaxakis, A. Manousakis-katsikakis, A. Panagiotou, I. Papavergou, N. Saoulidou, A. Stakia, K. Theofilatos, K. Vellidis, E. Vourliotis

National Technical University of Athens, Athens, Greece

G. Bakas, K. Kousouris, I. Papakrivopoulos, G. Tsipolitis

University of Ioánnina, Ioánnina, Greece

I. Evangelou, C. Foudas, P. Gianneios, P. Katsoulis, P. Kokkas, S. Mallios, K. Manitara, N. Manthos, I. Papadopoulos, J. Strologas, F.A. Triantis, D. Tsitsonis

MTA-ELTE Lendület CMS Particle and Nuclear Physics Group, Eötvös Loránd University, Budapest, Hungary

M. Bartók[22], R. Chudasama, M. Csanad, P. Major, K. Mandal, A. Mehta, M.I. Nagy, G. Pasztor, O. Surányi, G.I. Veres

Wigner Research Centre for Physics, Budapest, Hungary

G. Bencze, C. Hajdu, D. Horvath[23], F. Sikler, T.Á. Vámi, V. Veszpremi, G. Vesztergombi[†]

Institute of Nuclear Research ATOMKI, Debrecen, Hungary

N. Beni, S. Czellar, J. Karancsi[22], A. Makovec, J. Molnar, Z. Szillasi

Institute of Physics, University of Debrecen, Debrecen, Hungary

P. Raics, D. Teyssier, Z.L. Trocsanyi, B. Ujvari

Eszterhazy Karoly University, Karoly Robert Campus, Gyongyos, Hungary

T. Csorgo, W.J. Metzger, F. Nemes, T. Novak

Indian Institute of Science (IISc), Bangalore, India

S. Choudhury, J.R. Komaragiri, P.C. Tiwari

National Institute of Science Education and Research, HBNI, Bhubaneswar, India

S. Bahinipati[25], C. Kar, G. Kole, P. Mal, V.K. Muraleedharan Nair Bindhu, A. Nayak[26], D.K. Sahoo[25], S.K. Swain

JHEP06(2020)076

Panjab University, Chandigarh, India
S. Bansal, S.B. Beri, V. Bhatnagar, S. Chauhan, R. Chawla, N. Dhingra, R. Gupta, A. Kaur, M. Kaur, S. Kaur, P. Kumari, M. Lohan, M. Meena, K. Sandeep, S. Sharma, J.B. Singh, A.K. Virdi, G. Walia

University of Delhi, Delhi, India
A. Bhardwaj, B.C. Choudhary, R.B. Garg, M. Gola, S. Keshri, Ashok Kumar, M. Naimuddin, P. Priyanka, K. Ranjan, Aashaq Shah, R. Sharma

Saha Institute of Nuclear Physics, HBNI, Kolkata, India
R. Bhardwaj[27], M. Bharti[27], R. Bhattacharya, S. Bhattacharya, U. Bhawandeep[27], D. Bhowmik, S. Dutta, S. Ghosh, M. Maity[28], K. Mondal, S. Nandan, A. Purohit, P.K. Rout, G. Saha, S. Sarkar, T. Sarkar[28], M. Sharan, B. Singh[27], S. Thakur[27]

Indian Institute of Technology Madras, Madras, India
P.K. Behera, P. Kalbhor, A. Muhammad, P.R. Pujahari, A. Sharma, A.K. Sikdar

Bhabha Atomic Research Centre, Mumbai, India
D. Dutta, V. Jha, V. Kumar, D.K. Mishra, P.K. Netrakanti, L.M. Pant, P. Shukla

Tata Institute of Fundamental Research-A, Mumbai, India
T. Aziz, M.A. Bhat, S. Dugad, G.B. Mohanty, N. Sur, RavindraKumar Verma

Tata Institute of Fundamental Research-B, Mumbai, India
S. Banerjee, S. Bhattacharya, S. Chatterjee, P. Das, M. Guchait, S. Karmakar, S. Kumar, G. Majumder, K. Mazumdar, N. Sahoo, S. Sawant

Indian Institute of Science Education and Research (IISER), Pune, India
S. Dube, V. Hegde, B. Kansal, A. Kapoor, K. Kothekar, S. Pandey, A. Rane, A. Rastogi, S. Sharma

Institute for Research in Fundamental Sciences (IPM), Tehran, Iran
S. Chenarani[29], E. Eskandari Tadavani, S.M. Etesami[29], M. Khakzad, M. Mohammadi Najafabadi, M. Naseri, F. Rezaei Hosseinabadi

University College Dublin, Dublin, Ireland
M. Felcini, M. Grunewald

INFN Sezione di Bari[a], Università di Bari[b], Politecnico di Bari[c], Bari, Italy
M. Abbrescia[a,b], R. Aly[a,b,30], C. Calabria[a,b], A. Colaleo[a], D. Creanza[a,c], L. Cristella[a,b], N. De Filippis[a,c], M. De Palma[a,b], A. Di Florio[a,b], W. Elmetenawee[a,b], L. Fiore[a], A. Gelmi[a,b], G. Iaselli[a,c], M. Ince[a,b], S. Lezki[a,b], G. Maggi[a,c], M. Maggi[a], G. Miniello[a,b], S. My[a,b], S. Nuzzo[a,b], A. Pompili[a,b], G. Pugliese[a,c], R. Radogna[a], A. Ranieri[a], G. Selvaggi[a,b], L. Silvestris[a], F.M. Simone[a,b], R. Venditti[a], P. Verwilligen[a]

INFN Sezione di Bologna[a], Università di Bologna[b], Bologna, Italy
G. Abbiendi[a], C. Battilana[a,b], D. Bonacorsi[a,b], L. Borgonovi[a,b], S. Braibant-Giacomelli[a,b], R. Campanini[a,b], P. Capiluppi[a,b], A. Castro[a,b], F.R. Cavallo[a], C. Ciocca[a], G. Codispoti[a,b], M. Cuffiani[a,b], G.M. Dallavalle[a], F. Fabbri[a], A. Fanfani[a,b], E. Fontanesi[a,b], P. Giacomelli[a],

JHEP06(2020)076

C. Grandi[a], L. Guiducci[a,b], F. Iemmi[a,b], S. Lo Meo[a,31], S. Marcellini[a], G. Masetti[a], F.L. Navarria[a,b], A. Perrotta[a], F. Primavera[a,b], A.M. Rossi[a,b], T. Rovelli[a,b], G.P. Siroli[a,b], N. Tosi[a]

INFN Sezione di Catania[a], Università di Catania[b], Catania, Italy

S. Albergo[a,b,32], S. Costa[a,b], A. Di Mattia[a], R. Potenza[a,b], A. Tricomi[a,b,32], C. Tuve[a,b]

INFN Sezione di Firenze[a], Università di Firenze[b], Firenze, Italy

G. Barbagli[a], A. Cassese[a], R. Ceccarelli[a,b], V. Ciulli[a,b], C. Civinini[a], R. D'Alessandro[a,b], E. Focardi[a,b], G. Latino[a,b], P. Lenzi[a,b], M. Meschini[a], S. Paoletti[a], G. Sguazzoni[a], L. Viliani[a]

INFN Laboratori Nazionali di Frascati, Frascati, Italy

L. Benussi, S. Bianco, D. Piccolo

INFN Sezione di Genova[a], Università di Genova[b], Genova, Italy

M. Bozzo[a,b], F. Ferro[a], R. Mulargia[a,b], E. Robutti[a], S. Tosi[a,b]

INFN Sezione di Milano-Bicocca[a], Università di Milano-Bicocca[b], Milano, Italy

A. Benaglia[a], A. Beschi[a,b], F. Brivio[a,b], V. Ciriolo[a,b,18], S. Di Guida[a,b,18], M.E. Dinardo[a,b], P. Dini[a], S. Gennai[a], A. Ghezzi[a,b], P. Govoni[a,b], L. Guzzi[a,b], M. Malberti[a], S. Malvezzi[a], D. Menasce[a], F. Monti[a,b], L. Moroni[a], M. Paganoni[a,b], D. Pedrini[a], S. Ragazzi[a,b], T. Tabarelli de Fatis[a,b], D. Zuolo[a,b]

INFN Sezione di Napoli[a], Università di Napoli 'Federico II'[b], Napoli, Italy, Università della Basilicata[c], Potenza, Italy, Università G. Marconi[d], Roma, Italy

S. Buontempo[a], N. Cavallo[a,c], A. De Iorio[a,b], A. Di Crescenzo[a,b], F. Fabozzi[a,c], F. Fienga[a], G. Galati[a], A.O.M. Iorio[a,b], L. Lista[a,b], S. Meola[a,d,18], P. Paolucci[a,18], B. Rossi[a], C. Sciacca[a,b], E. Voevodina[a,b]

INFN Sezione di Padova[a], Università di Padova[b], Padova, Italy, Università di Trento[c], Trento, Italy

P. Azzi[a], N. Bacchetta[a], D. Bisello[a,b], A. Boletti[a,b], A. Bragagnolo[a,b], R. Carlin[a,b], P. Checchia[a], P. De Castro Manzano[a], T. Dorigo[a], U. Dosselli[a], F. Gasparini[a,b], U. Gasparini[a,b], A. Gozzelino[a], S.Y. Hoh[a,b], P. Lujan[a], M. Margoni[a,b], A.T. Meneguzzo[a,b], J. Pazzini[a,b], M. Presilla[b], P. Ronchese[a,b], R. Rossin[a,b], F. Simonetto[a,b], A. Tiko[a], M. Tosi[a,b], M. Zanetti[a,b], P. Zotto[a,b], G. Zumerle[a,b]

INFN Sezione di Pavia[a], Università di Pavia[b], Pavia, Italy

A. Braghieri[a], D. Fiorina[a,b], P. Montagna[a,b], S.P. Ratti[a,b], V. Re[a], M. Ressegotti[a,b], C. Riccardi[a,b], P. Salvini[a], I. Vai[a], P. Vitulo[a,b]

INFN Sezione di Perugia[a], Università di Perugia[b], Perugia, Italy

M. Biasini[a,b], G.M. Bilei[a], D. Ciangottini[a,b], L. Fanò[a,b], P. Lariccia[a,b], R. Leonardi[a,b], E. Manoni[a], G. Mantovani[a,b], V. Mariani[a,b], M. Menichelli[a], A. Rossi[a,b], A. Santocchia[a,b], D. Spiga[a]

JHEP06(2020)076

INFN Sezione di Pisa[a], Università di Pisa[b], Scuola Normale Superiore di Pisa[c], Pisa, Italy

K. Androsov[a], P. Azzurri[a], G. Bagliesi[a], V. Bertacchi[a,c], L. Bianchini[a], T. Boccali[a], R. Castaldi[a], M.A. Ciocci[a,b], R. Dell'Orso[a], G. Fedi[a], L. Giannini[a,c], A. Giassi[a], M.T. Grippo[a], F. Ligabue[a,c], E. Manca[a,c], G. Mandorli[a,c], A. Messineo[a,b], F. Palla[a], A. Rizzi[a,b], G. Rolandi[33], S. Roy Chowdhury, A. Scribano[a], P. Spagnolo[a], R. Tenchini[a], G. Tonelli[a,b], N. Turini[a], A. Venturi[a], P.G. Verdini[a]

INFN Sezione di Roma[a], Sapienza Università di Roma[b], Rome, Italy

F. Cavallari[a], M. Cipriani[a,b], D. Del Re[a,b], E. Di Marco[a,b], M. Diemoz[a], E. Longo[a,b], P. Meridiani[a], G. Organtini[a,b], F. Pandolfi[a], R. Paramatti[a,b], C. Quaranta[a,b], S. Rahatlou[a,b], C. Rovelli[a], F. Santanastasio[a,b], L. Soffi[a,b]

INFN Sezione di Torino[a], Università di Torino[b], Torino, Italy, Università del Piemonte Orientale[c], Novara, Italy

N. Amapane[a,b], R. Arcidiacono[a,c], S. Argiro[a,b], M. Arneodo[a,c], N. Bartosik[a], R. Bellan[a,b], A. Bellora, C. Biino[a], A. Cappati[a,b], N. Cartiglia[a], S. Cometti[a], M. Costa[a,b], R. Covarelli[a,b], N. Demaria[a], B. Kiani[a,b], C. Mariotti[a], S. Maselli[a], E. Migliore[a,b], V. Monaco[a,b], E. Monteil[a,b], M. Monteno[a], M.M. Obertino[a,b], G. Ortona[a,b], L. Pacher[a,b], N. Pastrone[a], M. Pelliccioni[a], G.L. Pinna Angioni[a,b], A. Romero[a,b], M. Ruspa[a,c], R. Salvatico[a,b], V. Sola[a], A. Solano[a,b], D. Soldi[a,b], A. Staiano[a]

INFN Sezione di Trieste[a], Università di Trieste[b], Trieste, Italy

S. Belforte[a], V. Candelise[a,b], M. Casarsa[a], F. Cossutti[a], A. Da Rold[a,b], G. Della Ricca[a,b], F. Vazzoler[a,b], A. Zanetti[a]

Kyungpook National University, Daegu, Korea

B. Kim, D.H. Kim, G.N. Kim, J. Lee, S.W. Lee, C.S. Moon, Y.D. Oh, S.I. Pak, S. Sekmen, D.C. Son, Y.C. Yang

Chonnam National University, Institute for Universe and Elementary Particles, Kwangju, Korea

H. Kim, D.H. Moon, G. Oh

Hanyang University, Seoul, Korea

B. Francois, T.J. Kim, J. Park

Korea University, Seoul, Korea

S. Cho, S. Choi, Y. Go, S. Ha, B. Hong, K. Lee, K.S. Lee, J. Lim, J. Park, S.K. Park, Y. Roh, J. Yoo

Kyung Hee University, Department of Physics

J. Goh

Sejong University, Seoul, Korea

H.S. Kim

JHEP06(2020)076

Seoul National University, Seoul, Korea
J. Almond, J.H. Bhyun, J. Choi, S. Jeon, J. Kim, J.S. Kim, H. Lee, K. Lee, S. Lee, K. Nam, M. Oh, S.B. Oh, B.C. Radburn-Smith, U.K. Yang, H.D. Yoo, I. Yoon, G.B. Yu

University of Seoul, Seoul, Korea
D. Jeon, H. Kim, J.H. Kim, J.S.H. Lee, I.C. Park, I.J Watson

Sungkyunkwan University, Suwon, Korea
Y. Choi, C. Hwang, Y. Jeong, J. Lee, Y. Lee, I. Yu

Riga Technical University, Riga, Latvia
V. Veckalns[34]

Vilnius University, Vilnius, Lithuania
V. Dudenas, A. Juodagalvis, A. Rinkevicius, G. Tamulaitis, J. Vaitkus

National Centre for Particle Physics, Universiti Malaya, Kuala Lumpur, Malaysia
Z.A. Ibrahim, F. Mohamad Idris[35], W.A.T. Wan Abdullah, M.N. Yusli, Z. Zolkapli

Universidad de Sonora (UNISON), Hermosillo, Mexico
J.F. Benitez, A. Castaneda Hernandez, J.A. Murillo Quijada, L. Valencia Palomo

Centro de Investigacion y de Estudios Avanzados del IPN, Mexico City, Mexico
H. Castilla-Valdez, E. De La Cruz-Burelo, I. Heredia-De La Cruz[36], R. Lopez-Fernandez, A. Sanchez-Hernandez

Universidad Iberoamericana, Mexico City, Mexico
S. Carrillo Moreno, C. Oropeza Barrera, M. Ramirez-Garcia, F. Vazquez Valencia

Benemerita Universidad Autonoma de Puebla, Puebla, Mexico
J. Eysermans, I. Pedraza, H.A. Salazar Ibarguen, C. Uribe Estrada

Universidad Autónoma de San Luis Potosí, San Luis Potosí, Mexico
A. Morelos Pineda

University of Montenegro, Podgorica, Montenegro
J. Mijuskovic, N. Raicevic

University of Auckland, Auckland, New Zealand
D. Krofcheck

University of Canterbury, Christchurch, New Zealand
S. Bheesette, P.H. Butler

National Centre for Physics, Quaid-I-Azam University, Islamabad, Pakistan
A. Ahmad, M. Ahmad, Q. Hassan, H.R. Hoorani, W.A. Khan, M.A. Shah, M. Shoaib, M. Waqas

AGH University of Science and Technology Faculty of Computer Science, Electronics and Telecommunications, Krakow, Poland
V. Avati, L. Grzanka, M. Malawski

JHEP06(2020)076

National Centre for Nuclear Research, Swierk, Poland
H. Bialkowska, M. Bluj, B. Boimska, M. Górski, M. Kazana, M. Szleper, P. Zalewski

Institute of Experimental Physics, Faculty of Physics, University of Warsaw, Warsaw, Poland
K. Bunkowski, A. Byszuk[37], K. Doroba, A. Kalinowski, M. Konecki, J. Krolikowski, M. Misiura, M. Olszewski, M. Walczak

Laboratório de Instrumentação e Física Experimental de Partículas, Lisboa, Portugal
M. Araujo, P. Bargassa, D. Bastos, A. Di Francesco, P. Faccioli, B. Galinhas, M. Gallinaro, J. Hollar, N. Leonardo, T. Niknejad, J. Seixas, K. Shchelina, G. Strong, O. Toldaiev, J. Varela

Joint Institute for Nuclear Research, Dubna, Russia
S. Afanasiev, P. Bunin, M. Gavrilenko, I. Golutvin, I. Gorbunov, A. Kamenev, V. Karjavine, A. Lanev, A. Malakhov, V. Matveev[38,39], P. Moisenz, V. Palichik, V. Perelygin, M. Savina, S. Shmatov, S. Shulha, N. Skatchkov, V. Smirnov, N. Voytishin, A. Zarubin

Petersburg Nuclear Physics Institute, Gatchina (St. Petersburg), Russia
L. Chtchipounov, V. Golovtcov, Y. Ivanov, V. Kim[40], E. Kuznetsova[41], P. Levchenko, V. Murzin, V. Oreshkin, I. Smirnov, D. Sosnov, V. Sulimov, L. Uvarov, A. Vorobyev

Institute for Nuclear Research, Moscow, Russia
Yu. Andreev, A. Dermenev, S. Gninenko, N. Golubev, A. Karneyeu, M. Kirsanov, N. Krasnikov, A. Pashenkov, D. Tlisov, A. Toropin

Institute for Theoretical and Experimental Physics named by A.I. Alikhanov of NRC 'Kurchatov Institute', Moscow, Russia
V. Epshteyn, V. Gavrilov, N. Lychkovskaya, A. Nikitenko[42], V. Popov, I. Pozdnyakov, G. Safronov, A. Spiridonov, A. Stepennov, M. Toms, E. Vlasov, A. Zhokin

Moscow Institute of Physics and Technology, Moscow, Russia
T. Aushev

National Research Nuclear University 'Moscow Engineering Physics Institute' (MEPhI), Moscow, Russia
M. Chadeeva[43], P. Parygin, D. Philippov, E. Popova, V. Rusinov

P.N. Lebedev Physical Institute, Moscow, Russia
V. Andreev, M. Azarkin, I. Dremin, M. Kirakosyan, A. Terkulov

Skobeltsyn Institute of Nuclear Physics, Lomonosov Moscow State University, Moscow, Russia
A. Belyaev, E. Boos, M. Dubinin[44], L. Dudko, A. Ershov, A. Gribushin, V. Klyukhin, O. Kodolova, I. Lokhtin, S. Obraztsov, S. Petrushanko, V. Savrin, A. Snigirev

Novosibirsk State University (NSU), Novosibirsk, Russia
A. Barnyakov[45], V. Blinov[45], T. Dimova[45], L. Kardapoltsev[45], Y. Skovpen[45]

JHEP06(2020)076

Institute for High Energy Physics of National Research Centre 'Kurchatov Institute', Protvino, Russia

I. Azhgirey, I. Bayshev, S. Bitioukov, V. Kachanov, D. Konstantinov, P. Mandrik, V. Petrov, R. Ryutin, S. Slabospitskii, A. Sobol, S. Troshin, N. Tyurin, A. Uzunian, A. Volkov

National Research Tomsk Polytechnic University, Tomsk, Russia

A. Babaev, A. Iuzhakov, V. Okhotnikov

Tomsk State University, Tomsk, Russia

V. Borchsh, V. Ivanchenko, E. Tcherniaev

University of Belgrade: Faculty of Physics and VINCA Institute of Nuclear Sciences

P. Adzic[46], P. Cirkovic, M. Dordevic, P. Milenovic, J. Milosevic, M. Stojanovic

Centro de Investigaciones Energéticas Medioambientales y Tecnológicas (CIEMAT), Madrid, Spain

M. Aguilar-Benitez, J. Alcaraz Maestre, A. Álvarez Fernández, I. Bachiller, M. Barrio Luna, J.A. Brochero Cifuentes, C.A. Carrillo Montoya, M. Cepeda, M. Cerrada, N. Colino, B. De La Cruz, A. Delgado Peris, C. Fernandez Bedoya, J.P. Fernández Ramos, J. Flix, M.C. Fouz, O. Gonzalez Lopez, S. Goy Lopez, J.M. Hernandez, M.I. Josa, D. Moran, Á. Navarro Tobar, A. Pérez-Calero Yzquierdo, J. Puerta Pelayo, I. Redondo, L. Romero, S. Sánchez Navas, M.S. Soares, A. Triossi, C. Willmott

Universidad Autónoma de Madrid, Madrid, Spain

C. Albajar, J.F. de Trocóniz, R. Reyes-Almanza

Universidad de Oviedo, Instituto Universitario de Ciencias y Tecnologías Espaciales de Asturias (ICTEA), Oviedo, Spain

B. Alvarez Gonzalez, J. Cuevas, C. Erice, J. Fernandez Menendez, S. Folgueras, I. Gonzalez Caballero, J.R. González Fernández, E. Palencia Cortezon, V. Rodríguez Bouza, S. Sanchez Cruz

Instituto de Física de Cantabria (IFCA), CSIC-Universidad de Cantabria, Santander, Spain

I.J. Cabrillo, A. Calderon, B. Chazin Quero, J. Duarte Campderros, M. Fernandez, P.J. Fernández Manteca, A. García Alonso, G. Gomez, C. Martinez Rivero, P. Martinez Ruiz del Arbol, F. Matorras, J. Piedra Gomez, C. Prieels, T. Rodrigo, A. Ruiz-Jimeno, L. Russo[47], L. Scodellaro, I. Vila, J.M. Vizan Garcia

University of Colombo, Colombo, Sri Lanka

D.U.J. Sonnadara

University of Ruhuna, Department of Physics, Matara, Sri Lanka

W.G.D. Dharmaratna, N. Wickramage

JHEP06(2020)076

CERN, European Organization for Nuclear Research, Geneva, Switzerland

D. Abbaneo, B. Akgun, E. Auffray, G. Auzinger, J. Baechler, P. Baillon, A.H. Ball, D. Barney, J. Bendavid, M. Bianco, A. Bocci, P. Bortignon, E. Bossini, C. Botta, E. Brondolin, T. Camporesi, A. Caratelli, G. Cerminara, E. Chapon, G. Cucciati, D. d'Enterria, A. Dabrowski, N. Daci, V. Daponte, A. David, O. Davignon, A. De Roeck, M. Deile, M. Dobson, M. Dünser, N. Dupont, A. Elliott-Peisert, N. Emriskova, F. Fallavollita[48], D. Fasanella, S. Fiorendi, G. Franzoni, J. Fulcher, W. Funk, S. Giani, D. Gigi, A. Gilbert, K. Gill, F. Glege, L. Gouskos, M. Gruchala, M. Guilbaud, D. Gulhan, J. Hegeman, C. Heidegger, Y. Iiyama, V. Innocente, T. James, P. Janot, O. Karacheban[21], J. Kaspar, J. Kieseler, M. Krammer[1], N. Kratochwil, C. Lange, P. Lecoq, C. Lourenço, L. Malgeri, M. Mannelli, A. Massironi, F. Meijers, J.A. Merlin, S. Mersi, E. Meschi, F. Moortgat, M. Mulders, J. Ngadiuba, J. Niedziela, S. Nourbakhsh, S. Orfanelli, L. Orsini, F. Pantaleo[18], L. Pape, E. Perez, M. Peruzzi, A. Petrilli, G. Petrucciani, A. Pfeiffer, M. Pierini, F.M. Pitters, D. Rabady, A. Racz, M. Rieger, M. Rovere, H. Sakulin, C. Schäfer, C. Schwick, M. Selvaggi, A. Sharma, P. Silva, W. Snoeys, P. Sphicas[49], J. Steggemann, S. Summers, V.R. Tavolaro, D. Treille, A. Tsirou, G.P. Van Onsem, A. Vartak, M. Verzetti, W.D. Zeuner

Paul Scherrer Institut, Villigen, Switzerland

L. Caminada[50], K. Deiters, W. Erdmann, R. Horisberger, Q. Ingram, H.C. Kaestli, D. Kotlinski, U. Langenegger, T. Rohe, S.A. Wiederkehr

ETH Zurich — Institute for Particle Physics and Astrophysics (IPA), Zurich, Switzerland

M. Backhaus, P. Berger, N. Chernyavskaya, G. Dissertori, M. Dittmar, M. Donegà, C. Dorfer, T.A. Gómez Espinosa, C. Grab, D. Hits, T. Klijnsma, W. Lustermann, R.A. Manzoni, M.T. Meinhard, F. Micheli, P. Musella, F. Nessi-Tedaldi, F. Pauss, G. Perrin, L. Perrozzi, S. Pigazzini, M.G. Ratti, M. Reichmann, C. Reissel, T. Reitenspiess, D. Ruini, D.A. Sanz Becerra, M. Schönenberger, L. Shchutska, M.L. Vesterbacka Olsson, R. Wallny, D.H. Zhu

Universität Zürich, Zurich, Switzerland

T.K. Aarrestad, C. Amsler[51], D. Brzhechko, M.F. Canelli, A. De Cosa, R. Del Burgo, S. Donato, B. Kilminster, S. Leontsinis, V.M. Mikuni, I. Neutelings, G. Rauco, P. Robmann, K. Schweiger, C. Seitz, Y. Takahashi, S. Wertz, A. Zucchetta

National Central University, Chung-Li, Taiwan

T.H. Doan, C.M. Kuo, W. Lin, A. Roy, S.S. Yu

National Taiwan University (NTU), Taipei, Taiwan

P. Chang, Y. Chao, K.F. Chen, P.H. Chen, W.-S. Hou, Y.y. Li, R.-S. Lu, E. Paganis, A. Psallidas, A. Steen

Chulalongkorn University, Faculty of Science, Department of Physics, Bangkok, Thailand

B. Asavapibhop, C. Asawatangtrakuldee, N. Srimanobhas, N. Suwonjandee

JHEP06(2020)076

Çukurova University, Physics Department, Science and Art Faculty, Adana, Turkey

A. Bat, F. Boran, A. Celik[52], S. Cerci[53], S. Damarseckin[54], Z.S. Demiroglu, F. Dolek, C. Dozen[55], I. Dumanoglu, G. Gokbulut, EmineGurpinar Guler[56], Y. Guler, I. Hos[57], C. Isik, E.E. Kangal[58], O. Kara, A. Kayis Topaksu, U. Kiminsu, G. Onengut, K. Ozdemir[59], S. Ozturk[60], A.E. Simsek, D. Sunar Cerci[53], U.G. Tok, S. Turkcapar, I.S. Zorbakir, C. Zorbilmez

Middle East Technical University, Physics Department, Ankara, Turkey

B. Isildak[61], G. Karapinar[62], M. Yalvac

Bogazici University, Istanbul, Turkey

I.O. Atakisi, E. Gülmez, M. Kaya[63], O. Kaya[64], Ö. Özçelik, S. Tekten, E.A. Yetkin[65]

Istanbul Technical University, Istanbul, Turkey

A. Cakir, K. Cankocak, Y. Komurcu, S. Sen[66]

Istanbul University, Istanbul, Turkey

B. Kaynak, S. Ozkorucuklu

Institute for Scintillation Materials of National Academy of Science of Ukraine, Kharkov, Ukraine

B. Grynyov

National Scientific Center, Kharkov Institute of Physics and Technology, Kharkov, Ukraine

L. Levchuk

University of Bristol, Bristol, United Kingdom

E. Bhal, S. Bologna, J.J. Brooke, D. Burns[67], E. Clement, D. Cussans, H. Flacher, J. Goldstein, G.P. Heath, H.F. Heath, L. Kreczko, B. Krikler, S. Paramesvaran, B. Penning, T. Sakuma, S. Seif El Nasr-Storey, V.J. Smith, J. Taylor, A. Titterton

Rutherford Appleton Laboratory, Didcot, United Kingdom

K.W. Bell, A. Belyaev[68], C. Brew, R.M. Brown, D.J.A. Cockerill, J.A. Coughlan, K. Harder, S. Harper, J. Linacre, K. Manolopoulos, D.M. Newbold, E. Olaiya, D. Petyt, T. Reis, T. Schuh, C.H. Shepherd-Themistocleous, A. Thea, I.R. Tomalin, T. Williams, W.J. Womersley

Imperial College, London, United Kingdom

R. Bainbridge, P. Bloch, J. Borg, S. Breeze, O. Buchmuller, A. Bundock, GurpreetSingh CHAHAL[69], D. Colling, P. Dauncey, G. Davies, M. Della Negra, R. Di Maria, P. Everaerts, G. Hall, G. Iles, M. Komm, C. Laner, L. Lyons, A.-M. Magnan, S. Malik, A. Martelli, V. Milosevic, A. Morton, J. Nash[70], V. Palladino, M. Pesaresi, D.M. Raymond, A. Richards, A. Rose, E. Scott, C. Seez, A. Shtipliyski, M. Stoye, T. Strebler, A. Tapper, K. Uchida, T. Virdee[18], N. Wardle, D. Winterbottom, J. Wright, A.G. Zecchinelli, S.C. Zenz

JHEP06(2020)076

Brunel University, Uxbridge, United Kingdom

J.E. Cole, P.R. Hobson, A. Khan, P. Kyberd, C.K. Mackay, I.D. Reid, L. Teodorescu, S. Zahid

Baylor University, Waco, U.S.A.

K. Call, B. Caraway, J. Dittmann, K. Hatakeyama, C. Madrid, B. McMaster, N. Pastika, C. Smith

Catholic University of America, Washington, DC, U.S.A.

R. Bartek, A. Dominguez, R. Uniyal, A.M. Vargas Hernandez

The University of Alabama, Tuscaloosa, U.S.A.

A. Buccilli, S.I. Cooper, C. Henderson, P. Rumerio, C. West

Boston University, Boston, U.S.A.

A. Albert, D. Arcaro, Z. Demiragli, D. Gastler, C. Richardson, J. Rohlf, D. Sperka, I. Suarez, L. Sulak, D. Zou

Brown University, Providence, U.S.A.

G. Benelli, B. Burkle, X. Coubez[19], D. Cutts, Y.t. Duh, M. Hadley, U. Heintz, J.M. Hogan[71], K.H.M. Kwok, E. Laird, G. Landsberg, K.T. Lau, J. Lee, Z. Mao, M. Narain, S. Sagir[72], R. Syarif, E. Usai, D. Yu, W. Zhang

University of California, Davis, Davis, U.S.A.

R. Band, C. Brainerd, R. Breedon, M. Calderon De La Barca Sanchez, M. Chertok, J. Conway, R. Conway, P.T. Cox, R. Erbacher, C. Flores, G. Funk, F. Jensen, W. Ko, O. Kukral, R. Lander, M. Mulhearn, D. Pellett, J. Pilot, M. Shi, D. Taylor, K. Tos, M. Tripathi, Z. Wang, F. Zhang

University of California, Los Angeles, U.S.A.

M. Bachtis, C. Bravo, R. Cousins, A. Dasgupta, A. Florent, J. Hauser, M. Ignatenko, N. Mccoll, W.A. Nash, S. Regnard, D. Saltzberg, C. Schnaible, B. Stone, V. Valuev

University of California, Riverside, Riverside, U.S.A.

K. Burt, Y. Chen, R. Clare, J.W. Gary, S.M.A. Ghiasi Shirazi, G. Hanson, G. Karapostoli, E. Kennedy, O.R. Long, M. Olmedo Negrete, M.I. Paneva, W. Si, L. Wang, S. Wimpenny, B.R. Yates, Y. Zhang

University of California, San Diego, La Jolla, U.S.A.

J.G. Branson, P. Chang, S. Cittolin, S. Cooperstein, N. Deelen, M. Derdzinski, R. Gerosa, D. Gilbert, B. Hashemi, D. Klein, V. Krutelyov, J. Letts, M. Masciovecchio, S. May, S. Padhi, M. Pieri, V. Sharma, M. Tadel, F. Würthwein, A. Yagil, G. Zevi Della Porta

University of California, Santa Barbara — Department of Physics, Santa Barbara, U.S.A.

N. Amin, R. Bhandari, C. Campagnari, M. Citron, V. Dutta, M. Franco Sevilla, J. Incandela, B. Marsh, H. Mei, A. Ovcharova, H. Qu, J. Richman, U. Sarica, D. Stuart, S. Wang

JHEP06(2020)076

California Institute of Technology, Pasadena, U.S.A.

D. Anderson, A. Bornheim, O. Cerri, I. Dutta, J.M. Lawhorn, N. Lu, J. Mao, H.B. Newman, T.Q. Nguyen, J. Pata, M. Spiropulu, J.R. Vlimant, S. Xie, Z. Zhang, R.Y. Zhu

Carnegie Mellon University, Pittsburgh, U.S.A.

M.B. Andrews, T. Ferguson, T. Mudholkar, M. Paulini, M. Sun, I. Vorobiev, M. Weinberg

University of Colorado Boulder, Boulder, U.S.A.

J.P. Cumalat, W.T. Ford, E. MacDonald, T. Mulholland, R. Patel, A. Perloff, K. Stenson, K.A. Ulmer, S.R. Wagner

Cornell University, Ithaca, U.S.A.

J. Alexander, Y. Cheng, J. Chu, A. Datta, A. Frankenthal, K. Mcdermott, J.R. Patterson, D. Quach, A. Ryd, S.M. Tan, Z. Tao, J. Thom, P. Wittich, M. Zientek

Fermi National Accelerator Laboratory, Batavia, U.S.A.

S. Abdullin, M. Albrow, M. Alyari, G. Apollinari, A. Apresyan, A. Apyan, S. Banerjee, L.A.T. Bauerdick, A. Beretvas, D. Berry, J. Berryhill, P.C. Bhat, K. Burkett, J.N. Butler, A. Canepa, G.B. Cerati, H.W.K. Cheung, F. Chlebana, M. Cremonesi, J. Duarte, V.D. Elvira, J. Freeman, Z. Gecse, E. Gottschalk, L. Gray, D. Green, S. Grünendahl, O. Gutsche, AllisonReinsvold Hall, J. Hanlon, R.M. Harris, S. Hasegawa, R. Heller, J. Hirschauer, B. Jayatilaka, S. Jindariani, M. Johnson, U. Joshi, B. Klima, M.J. Kortelainen, B. Kreis, S. Lammel, J. Lewis, D. Lincoln, R. Lipton, M. Liu, T. Liu, J. Lykken, K. Maeshima, J.M. Marraffino, D. Mason, P. McBride, P. Merkel, S. Mrenna, S. Nahn, V. O'Dell, V. Papadimitriou, K. Pedro, C. Pena, G. Rakness, F. Ravera, L. Ristori, B. Schneider, E. Sexton-Kennedy, N. Smith, A. Soha, W.J. Spalding, L. Spiegel, S. Stoynev, J. Strait, N. Strobbe, L. Taylor, S. Tkaczyk, N.V. Tran, L. Uplegger, E.W. Vaandering, C. Vernieri, R. Vidal, M. Wang, H.A. Weber

University of Florida, Gainesville, U.S.A.

D. Acosta, P. Avery, D. Bourilkov, A. Brinkerhoff, L. Cadamuro, A. Carnes, V. Cherepanov, F. Errico, R.D. Field, S.V. Gleyzer, B.M. Joshi, M. Kim, J. Konigsberg, A. Korytov, K.H. Lo, P. Ma, K. Matchev, N. Menendez, G. Mitselmakher, D. Rosenzweig, K. Shi, J. Wang, S. Wang, X. Zuo

Florida International University, Miami, U.S.A.

Y.R. Joshi

Florida State University, Tallahassee, U.S.A.

T. Adams, A. Askew, S. Hagopian, V. Hagopian, K.F. Johnson, R. Khurana, T. Kolberg, G. Martinez, T. Perry, H. Prosper, C. Schiber, R. Yohay, J. Zhang

Florida Institute of Technology, Melbourne, U.S.A.

M.M. Baarmand, M. Hohlmann, D. Noonan, M. Rahmani, M. Saunders, F. Yumiceva

University of Illinois at Chicago (UIC), Chicago, U.S.A.

M.R. Adams, L. Apanasevich, R.R. Betts, R. Cavanaugh, X. Chen, S. Dittmer, O. Evdokimov, C.E. Gerber, D.A. Hangal, D.J. Hofman, K. Jung, C. Mills, T. Roy, M.B. Tonjes, N. Varelas, J. Viinikainen, H. Wang, X. Wang, Z. Wu

JHEP06(2020)076

The University of Iowa, Iowa City, U.S.A.

M. Alhusseini, B. Bilki[56], W. Clarida, K. Dilsiz[73], S. Durgut, R.P. Gandrajula, M. Haytmyradov, V. Khristenko, O.K. Köseyan, J.-P. Merlo, A. Mestvirishvili[74], A. Moeller, J. Nachtman, H. Ogul[75], Y. Onel, F. Ozok[76], A. Penzo, C. Snyder, E. Tiras, J. Wetzel

Johns Hopkins University, Baltimore, U.S.A.

B. Blumenfeld, A. Cocoros, N. Eminizer, A.V. Gritsan, W.T. Hung, S. Kyriacou, P. Maksimovic, J. Roskes, M. Swartz

The University of Kansas, Lawrence, U.S.A.

C. Baldenegro Barrera, P. Baringer, A. Bean, S. Boren, J. Bowen, A. Bylinkin, T. Isidori, S. Khalil, J. King, G. Krintiras, A. Kropivnitskaya, C. Lindsey, D. Majumder, W. Mcbrayer, N. Minafra, M. Murray, C. Rogan, C. Royon, S. Sanders, E. Schmitz, J.D. Tapia Takaki, Q. Wang, J. Williams, G. Wilson

Kansas State University, Manhattan, U.S.A.

S. Duric, A. Ivanov, K. Kaadze, D. Kim, Y. Maravin, D.R. Mendis, T. Mitchell, A. Modak, A. Mohammadi

Lawrence Livermore National Laboratory, Livermore, U.S.A.

F. Rebassoo, D. Wright

University of Maryland, College Park, U.S.A.

A. Baden, O. Baron, A. Belloni, S.C. Eno, Y. Feng, N.J. Hadley, S. Jabeen, G.Y. Jeng, R.G. Kellogg, J. Kunkle, A.C. Mignerey, S. Nabili, F. Ricci-Tam, M. Seidel, Y.H. Shin, A. Skuja, S.C. Tonwar, K. Wong

Massachusetts Institute of Technology, Cambridge, U.S.A.

D. Abercrombie, B. Allen, A. Baty, R. Bi, S. Brandt, W. Busza, I.A. Cali, M. D'Alfonso, G. Gomez Ceballos, M. Goncharov, P. Harris, D. Hsu, M. Hu, M. Klute, D. Kovalskyi, Y.-J. Lee, P.D. Luckey, B. Maier, A.C. Marini, C. Mcginn, C. Mironov, S. Narayanan, X. Niu, C. Paus, D. Rankin, C. Roland, G. Roland, Z. Shi, G.S.F. Stephans, K. Sumorok, K. Tatar, D. Velicanu, J. Wang, T.W. Wang, B. Wyslouch

University of Minnesota, Minneapolis, U.S.A.

R.M. Chatterjee, A. Evans, S. Guts†, P. Hansen, J. Hiltbrand, Sh. Jain, Y. Kubota, Z. Lesko, J. Mans, R. Rusack, M.A. Wadud

University of Mississippi, Oxford, U.S.A.

J.G. Acosta, S. Oliveros

University of Nebraska-Lincoln, Lincoln, U.S.A.

K. Bloom, S. Chauhan, D.R. Claes, C. Fangmeier, L. Finco, F. Golf, R. Kamalieddin, I. Kravchenko, J.E. Siado, G.R. Snow†, B. Stieger, W. Tabb

State University of New York at Buffalo, Buffalo, U.S.A.

G. Agarwal, C. Harrington, I. Iashvili, A. Kharchilava, C. McLean, D. Nguyen, A. Parker, J. Pekkanen, S. Rappoccio, B. Roozbahani

JHEP06(2020)076

Northeastern University, Boston, U.S.A.

G. Alverson, E. Barberis, C. Freer, Y. Haddad, A. Hortiangtham, G. Madigan, B. Marzocchi, D.M. Morse, T. Orimoto, L. Skinnari, A. Tishelman-Charny, T. Wamorkar, B. Wang, A. Wisecarver, D. Wood

Northwestern University, Evanston, U.S.A.

S. Bhattacharya, J. Bueghly, T. Gunter, K.A. Hahn, N. Odell, M.H. Schmitt, K. Sung, M. Trovato, M. Velasco

University of Notre Dame, Notre Dame, U.S.A.

R. Bucci, N. Dev, R. Goldouzian, M. Hildreth, K. Hurtado Anampa, C. Jessop, D.J. Karmgard, K. Lannon, W. Li, N. Loukas, N. Marinelli, I. Mcalister, F. Meng, C. Mueller, Y. Musienko[38], M. Planer, R. Ruchti, P. Siddireddy, G. Smith, S. Taroni, M. Wayne, A. Wightman, M. Wolf, A. Woodard

The Ohio State University, Columbus, U.S.A.

J. Alimena, B. Bylsma, L.S. Durkin, B. Francis, C. Hill, W. Ji, A. Lefeld, T.Y. Ling, B.L. Winer

Princeton University, Princeton, U.S.A.

G. Dezoort, P. Elmer, J. Hardenbrook, N. Haubrich, S. Higginbotham, A. Kalogeropoulos, S. Kwan, D. Lange, M.T. Lucchini, J. Luo, D. Marlow, K. Mei, I. Ojalvo, J. Olsen, C. Palmer, P. Piroué, J. Salfeld-Nebgen, D. Stickland, C. Tully, Z. Wang

University of Puerto Rico, Mayaguez, U.S.A.

S. Malik, S. Norberg

Purdue University, West Lafayette, U.S.A.

A. Barker, V.E. Barnes, S. Das, L. Gutay, M. Jones, A.W. Jung, A. Khatiwada, B. Mahakud, D.H. Miller, G. Negro, N. Neumeister, C.C. Peng, S. Piperov, H. Qiu, J.F. Schulte, N. Trevisani, F. Wang, R. Xiao, W. Xie

Purdue University Northwest, Hammond, U.S.A.

T. Cheng, J. Dolen, N. Parashar

Rice University, Houston, U.S.A.

U. Behrens, K.M. Ecklund, S. Freed, F.J.M. Geurts, M. Kilpatrick, Arun Kumar, W. Li, B.P. Padley, R. Redjimi, J. Roberts, J. Rorie, W. Shi, A.G. Stahl Leiton, Z. Tu, A. Zhang

University of Rochester, Rochester, U.S.A.

A. Bodek, P. de Barbaro, R. Demina, J.L. Dulemba, C. Fallon, T. Ferbel, M. Galanti, A. Garcia-Bellido, O. Hindrichs, A. Khukhunaishvili, E. Ranken, R. Taus

Rutgers, The State University of New Jersey, Piscataway, U.S.A.

B. Chiarito, J.P. Chou, A. Gandrakota, Y. Gershtein, E. Halkiadakis, A. Hart, M. Heindl, E. Hughes, S. Kaplan, I. Laflotte, A. Lath, R. Montalvo, K. Nash, M. Osherson, H. Saka, S. Salur, S. Schnetzer, S. Somalwar, R. Stone, S. Thomas

JHEP06(2020)076

University of Tennessee, Knoxville, U.S.A.

H. Acharya, A.G. Delannoy, S. Spanier

Texas A&M University, College Station, U.S.A.

O. Bouhali[77], M. Dalchenko, M. De Mattia, A. Delgado, S. Dildick, R. Eusebi, J. Gilmore, T. Huang, T. Kamon[78], S. Luo, S. Malhotra, D. Marley, R. Mueller, D. Overton, L. Perniè, D. Rathjens, A. Safonov

Texas Tech University, Lubbock, U.S.A.

N. Akchurin, J. Damgov, F. De Guio, S. Kunori, K. Lamichhane, S.W. Lee, T. Mengke, S. Muthumuni, T. Peltola, S. Undleeb, I. Volobouev, Z. Wang, A. Whitbeck

Vanderbilt University, Nashville, U.S.A.

S. Greene, A. Gurrola, R. Janjam, W. Johns, C. Maguire, A. Melo, H. Ni, K. Padeken, F. Romeo, P. Sheldon, S. Tuo, J. Velkovska, M. Verweij

University of Virginia, Charlottesville, U.S.A.

M.W. Arenton, P. Barria, B. Cox, G. Cummings, J. Hakala, R. Hirosky, M. Joyce, A. Ledovskoy, C. Neu, B. Tannenwald, Y. Wang, E. Wolfe, F. Xia

Wayne State University, Detroit, U.S.A.

R. Harr, P.E. Karchin, N. Poudyal, J. Sturdy, P. Thapa

University of Wisconsin — Madison, Madison, WI, U.S.A.

T. Bose, J. Buchanan, C. Caillol, D. Carlsmith, S. Dasu, I. De Bruyn, L. Dodd, F. Fiori, C. Galloni, B. Gomber[79], H. He, M. Herndon, A. Hervé, U. Hussain, P. Klabbers, A. Lanaro, A. Loeliger, K. Long, R. Loveless, J. Madhusudanan Sreekala, D. Pinna, T. Ruggles, A. Savin, V. Sharma, W.H. Smith, D. Teague, S. Trembath-reichert, N. Woods

†: Deceased
1: Also at Vienna University of Technology, Vienna, Austria
2: Also at IRFU, CEA, Université Paris-Saclay, Gif-sur-Yvette, France
3: Also at Universidade Estadual de Campinas, Campinas, Brazil
4: Also at Federal University of Rio Grande do Sul, Porto Alegre, Brazil
5: Also at UFMS, Nova Andradina, Brazil
6: Also at Universidade Federal de Pelotas, Pelotas, Brazil
7: Also at Université Libre de Bruxelles, Bruxelles, Belgium
8: Also at University of Chinese Academy of Sciences, Beijing, China
9: Also at Institute for Theoretical and Experimental Physics named by A.I. Alikhanov of NRC 'Kurchatov Institute', Moscow, Russia
10: Also at Joint Institute for Nuclear Research, Dubna, Russia
11: Also at Suez University, Suez, Egypt
12: Now at British University in Egypt, Cairo, Egypt
13: Also at Purdue University, West Lafayette, U.S.A.
14: Also at Université de Haute Alsace, Mulhouse, France
15: Also at Tbilisi State University, Tbilisi, Georgia
16: Also at Ilia State University, Tbilisi, Georgia
17: Also at Erzincan Binali Yildirim University, Erzincan, Turkey

JHEP06(2020)076

18: Also at CERN, European Organization for Nuclear Research, Geneva, Switzerland
19: Also at RWTH Aachen University, III. Physikalisches Institut A, Aachen, Germany
20: Also at University of Hamburg, Hamburg, Germany
21: Also at Brandenburg University of Technology, Cottbus, Germany
22: Also at Institute of Physics, University of Debrecen, Debrecen, Hungary, Debrecen, Hungary
23: Also at Institute of Nuclear Research ATOMKI, Debrecen, Hungary
24: Also at MTA-ELTE Lendület CMS Particle and Nuclear Physics Group, Eötvös Loránd University, Budapest, Hungary, Budapest, Hungary
25: Also at IIT Bhubaneswar, Bhubaneswar, India, Bhubaneswar, India
26: Also at Institute of Physics, Bhubaneswar, India
27: Also at Shoolini University, Solan, India
28: Also at University of Visva-Bharati, Santiniketan, India
29: Also at Isfahan University of Technology, Isfahan, Iran
30: Now at INFN Sezione di Bari[a], Università di Bari[b], Politecnico di Bari[c], Bari, Italy
31: Also at Italian National Agency for New Technologies, Energy and Sustainable Economic Development, Bologna, Italy
32: Also at Centro Siciliano di Fisica Nucleare e di Struttura Della Materia, Catania, Italy
33: Also at Scuola Normale e Sezione dell'INFN, Pisa, Italy
34: Also at Riga Technical University, Riga, Latvia, Riga, Latvia
35: Also at Malaysian Nuclear Agency, MOSTI, Kajang, Malaysia
36: Also at Consejo Nacional de Ciencia y Tecnología, Mexico City, Mexico
37: Also at Warsaw University of Technology, Institute of Electronic Systems, Warsaw, Poland
38: Also at Institute for Nuclear Research, Moscow, Russia
39: Now at National Research Nuclear University 'Moscow Engineering Physics Institute' (MEPhI), Moscow, Russia
40: Also at St. Petersburg State Polytechnical University, St. Petersburg, Russia
41: Also at University of Florida, Gainesville, U.S.A.
42: Also at Imperial College, London, United Kingdom
43: Also at P.N. Lebedev Physical Institute, Moscow, Russia
44: Also at California Institute of Technology, Pasadena, U.S.A.
45: Also at Budker Institute of Nuclear Physics, Novosibirsk, Russia
46: Also at Faculty of Physics, University of Belgrade, Belgrade, Serbia
47: Also at Università degli Studi di Siena, Siena, Italy
48: Also at INFN Sezione di Pavia[a], Università di Pavia[b], Pavia, Italy, Pavia, Italy
49: Also at National and Kapodistrian University of Athens, Athens, Greece
50: Also at Universität Zürich, Zurich, Switzerland
51: Also at Stefan Meyer Institute for Subatomic Physics, Vienna, Austria, Vienna, Austria
52: Also at Burdur Mehmet Akif Ersoy University, BURDUR, Turkey
53: Also at Adiyaman University, Adiyaman, Turkey
54: Also at Şırnak University, Sirnak, Turkey
55: Also at Department of Physics, Tsinghua University, Beijing, China, Beijing, China
56: Also at Beykent University, Istanbul, Turkey, Istanbul, Turkey
57: Also at Istanbul Aydin University, Application and Research Center for Advanced Studies (App. & Res. Cent. for Advanced Studies), Istanbul, Turkey
58: Also at Mersin University, Mersin, Turkey
59: Also at Piri Reis University, Istanbul, Turkey
60: Also at Gaziosmanpasa University, Tokat, Turkey
61: Also at Ozyegin University, Istanbul, Turkey

JHEP06(2020)076

62: Also at Izmir Institute of Technology, Izmir, Turkey
63: Also at Marmara University, Istanbul, Turkey
64: Also at Kafkas University, Kars, Turkey
65: Also at Istanbul Bilgi University, Istanbul, Turkey
66: Also at Hacettepe University, Ankara, Turkey
67: Also at Vrije Universiteit Brussel, Brussel, Belgium
68: Also at School of Physics and Astronomy, University of Southampton, Southampton, United Kingdom
69: Also at IPPP Durham University, Durham, United Kingdom
70: Also at Monash University, Faculty of Science, Clayton, Australia
71: Also at Bethel University, St. Paul, Minneapolis, U.S.A., St. Paul, U.S.A.
72: Also at Karamanoğlu Mehmetbey University, Karaman, Turkey
73: Also at Bingol University, Bingol, Turkey
74: Also at Georgian Technical University, Tbilisi, Georgia
75: Also at Sinop University, Sinop, Turkey
76: Also at Mimar Sinan University, Istanbul, Istanbul, Turkey
77: Also at Texas A&M University at Qatar, Doha, Qatar
78: Also at Kyungpook National University, Daegu, Korea, Daegu, Korea
79: Also at University of Hyderabad, Hyderabad, India

JHEP06(2020)076